





Article

Arabidopsis Transcriptomics Reveals the Role of Lipoygenase2 (AtLOX2) in Wound-Induced Responses

Diljot Kaur^{1,2}, Andreas Schedl^{3,4,5}, Christine Lafleur⁶, Julian Martinez Henao¹, Nicole M. van Dam^{3,4,7} , Jean Rivoal²  and Jacqueline C. Bede^{1,*}

- ¹ Department of Plant Science, McGill University, 21,111 rue Lakeshore, Ste-Anne-de-Bellevue, QC H9X 3V9, Canada; diljot.kaur@mail.mcgill.ca (D.K.); julian.martinezhenao@mail.mcgill.ca (J.M.H.)
- ² Institut de Recherche en Biologie Végétale, Université de Montréal, 4101 rue Sherbrooke E., Montréal, QC H1X 2B2, Canada; jean.rivoal@umontreal.ca
- ³ German Centre for Integrative Biodiversity Research (iDiv) Halle-Jena-Leipzig, Deutscher Platz 52, 04103 Leipzig, Germany; vandam@igzev.de (N.M.v.D.)
- ⁴ Institute of Biodiversity, Friedrich Schiller University Jena, 07743 Jena, Germany
- ⁵ German Biomass Research Centre (DBFZ), Torgauer Straße 116, 04347 Leipzig, Germany
- ⁶ Department of Animal Science, McGill University, 21,111 rue Lakeshore, Ste-Anne-de-Bellevue, QC H9X 3V9, Canada; christine.lafleur@mcgill.ca
- ⁷ Leibniz Institute for Vegetable and Ornamental Crops (IGZ), Theodor-Echtermeyerweg-1, 14979 Großbeeren, Germany
- * Correspondence: jacqueline.bede@mcgill.ca; Tel.: +1-514-398-7860; Fax: +1-514-398-7897

Abstract: In wounded *Arabidopsis thaliana* leaves, four 13S-lipoxygenases (AtLOX2, AtLOX3, AtLOX4, AtLOX6) act in a hierarchical manner to contribute to the jasmonate burst. This leads to defense responses with LOX2 playing an important role in plant resistance against caterpillar herbivory. In this study, we sought to characterize the impact of AtLOX2 on wound-induced phytohormonal and transcriptional responses to foliar mechanical damage using wildtype (WT) and *lox2* mutant plants. Compared with WT, the *lox2* mutant had higher constitutive levels of the phytohormone salicylic acid (SA) and enhanced expression of SA-responsive genes. This suggests that AtLOX2 may be involved in the biosynthesis of jasmonates that are involved in the antagonism of SA biosynthesis. As expected, the jasmonate burst in response to wounding was dampened in *lox2* plants. Generally, 1 h after wounding, genes linked to jasmonate biosynthesis, jasmonate signaling attenuation and abscisic acid-responsive genes, which are primarily involved in wound sealing and healing, were differentially regulated between WT and *lox2* mutants. Twelve h after wounding, WT plants showed stronger expression of genes associated with plant protection against insect herbivory. This study highlights the dynamic nature of jasmonate-responsive gene expression and the contribution of AtLOX2 to this pathway and plant resistance against insects.

Keywords: AtLOX2; jasmonate; 13S-lipoxygenase; transcriptome; wounding



Citation: Kaur, D.; Schedl, A.; Lafleur, C.; Martinez Henao, J.; van Dam, N.M.; Rivoal, J.; Bede, J.C. Arabidopsis Transcriptomics Reveals the Role of Lipoygenase2 (AtLOX2) in Wound-Induced Responses. *Int. J. Mol. Sci.* **2024**, *25*, 5898. <https://doi.org/10.3390/ijms25115898>

Academic Editor: Vladimir Zhurov

Received: 25 April 2024

Revised: 22 May 2024

Accepted: 24 May 2024

Published: 28 May 2024



Copyright: © 2024 by the authors. Licensee MDPI, Basel, Switzerland. This article is an open access article distributed under the terms and conditions of the Creative Commons Attribution (CC BY) license (<https://creativecommons.org/licenses/by/4.0/>).

1. Introduction

In addition to their roles in plant development, such as root elongation and pollen development [1,2], jasmonates are most recognized for their critical role in induced plant resistance to necrotrophic pathogens and chewing insect herbivores [3]. In *Arabidopsis thaliana* (arabidopsis), jasmonate biosynthesis is initiated from chloroplast membrane-derived galactolipids generating α -linolenic acid (18:3) upon wounding or recognition of pathogen or insect attack [1,4,5]. A stromal 13S-lipoxygenase (LOX) then catalyzes the oxygenation of α -linolenic acid at the 13C position, producing (13S)-hydroperoxyoctadecatrienoic acid (HPOA). Through sequential reactions catalyzed by allene oxide synthase (AOS) and allene oxide cyclase (AOC), HPOA is converted to the active phytohormone (9S,13S)-12-oxo-phytodienoic acid (OPDA), which is transported from the chloroplast by JASSY transporters [6–8]. Through the CTS/PXA1 transporters [9], OPDA is transported from

the chloroplast to the peroxisome and converted to jasmonic acid (JA) through reduction followed by β -oxidation. JA is exported to the cytosol, possibly through the transporter AtJAT2 [10], where it is conjugated to isoleucine, a step catalyzed by jasmonate-resistant 1 (JAR1) [11], to form the bioactive (+)-7-*iso*-jasmonoyl-isoleucine (JA-Ile) [12]. The resultant JA-Ile enters the nucleus via AtJAT1 to bridge jasmonate-ZIM domain (JAZ) transcriptional repressors to the SCF^{COI1} complex that ubiquitinates the JAZ protein, targeting them for degradation by the 26S-proteasome [13–15]. Removal of JAZ proteins releases MYC transcription factors from the JAZ-NINJA-TOPLESS repressor complex, allowing MED25 to interact with the MYC transcription factors and jasmonate-responsive transcript expression to occur, leading to gene expression involved in plant defenses [16,17].

In arabidopsis, jasmonate signaling leads increased foliar levels of glucosinolates (GSLs), S- and N-rich specialized metabolites that contribute protection against insects and pathogens [18–20]. In the leaves, GSLs are spatially separated from their activating enzyme, myrosinase [21]. Herbivore damage disrupting foliar tissue allows contact between the myrosinases and GSLs, resulting in the hydrolysis of the thioester bond and releasing an unstable compound that undergoes rearrangement to produce toxic compounds such as isothiocyanates, thiocyanates and nitriles [18]. Though both aliphatic and indolic GSLs may negatively affect insect herbivores, in general, aliphatic GSLs have a stronger negative impact on generalist caterpillar herbivores while indolic GSLs negatively affect aphids [22–26].

Given the increase in jasmonates within seconds after wounding [27,28], jasmonate biosynthetic enzymes are thought to be constitutively present and regulated both transcriptionally and post-translationally in response to stress [29,30]. Indeed, an enzyme that catalyzes an early step in jasmonate biosynthesis, AtLOX2, is constitutively phosphorylated at Ser⁶⁰⁰ and dephosphorylated in wounded plants [31]. In vitro studies using phosphovariants confirmed that phosphorylation of AtLOX2 at Ser⁶⁰⁰ may affect enzyme activity with lower activity observed in the phosphomimics (Ser⁶⁰⁰-to-Asp, Ser⁶⁰⁰-to-Met) compared with the unphosphorylated WT (Ser⁶⁰⁰) or phosphonull variants (Ser⁶⁰⁰-to-Ala) [32]. This is likely due to the fact that Ser⁶⁰⁰ phosphorylation interferes with the positioning of the substrate on the enzyme active site.

13S-LOXs, such as AtLOX2, catalyze the addition of oxygen to the 13-position of a chloroplast membrane-derived polyunsaturated fatty acid, typically α -linolenic acid. In arabidopsis, there are four functional 13S-LOXs, AtLOX2, AtLOX3, AtLOX4 and AtLOX6, that contribute to the jasmonate burst. A hierarchy is noted where LOX2 and LOX6 activity results in jasmonate production that leads to the expression of *AtLOX2*, *AtLOX3* and *AtLOX4* [33]. Thus, AtLOX2 contributes to the early foliar jasmonate burst, as does AtLOX6, and is primarily associated with mesophyll and bundle sheath cells and important in local signaling [27,28,33]. In contrast, AtLOX6 is localized near the vasculature and likely plays an important role in long-range jasmonate signals. AtLOX3 and AtLOX4 are associated with the xylem and phloem, respectively, and are responsible for later (4 h after wounding) jasmonate biosynthesis, along with AtLOX2.

Even though these four functional AtLOXs contribute to jasmonate biosynthesis in response to plant stress, AtLOX2 is thought to be the most important for plant resistance against caterpillar herbivory [28,33]. Generalist caterpillars of the Egyptian cotton leafworm, *Spodoptera littoralis*, gained nearly twice the biomass when reared on the *lox2* mutant compared with WT or *lox3/4/6* plants [33]. As well, LOX2 activity results in singlet oxygen (¹O₂) production in wounded leaf tissue, which may affect transcriptional responses [34,35].

In this study, we seek to dissect the role of AtLOX2 in plant defense further by comparing wound-induced responses after foliar wounding of Col-0 and the loss-of-function *lox2* mutant. We combined bioinformatic analyses of transcriptomics data with phytohormone and GSL analyses focusing on phytohormone signaling and ¹O₂-responsive gene expression as well as GSL metabolism. Our results show that constitutive AtLOX2-associated jasmonate biosynthesis may be involved in antagonizing salicylic acid (SA) levels. In wounded arabidopsis, AtLOX2 exerts a high degree of control on the plants' response to

damage. In particular, the mechanically damage-associated jasmonate burst was lower in the *lox2* mutant, which is reflected in the reduced expression of late wound-induced genes.

2. Results

Arabidopsis has four functional 13S-LOXs involved in the biosynthesis of jasmonates in response to wounding or biotic stresses, such as insect herbivory or pathogens, making it complex to tease out the role of individual enzymes in plant resistance [36]. In wounded *Arabidopsis* leaves, these proteins work in a hierarchical arrangement with AtLOX2, primarily contributing to plant resistance against caterpillar herbivory [33]. Using a *lox2* mutant [28], we conducted a time course transcriptomic experiment to understand the role of AtLOX2 in the plant response to wounding, particularly in connection to plant protection.

2.1. Transcriptome Profiling and Mapping onto the *Arabidopsis* Genome

After processing to remove the adaptor and poor-quality reads, RNA-Seq produced an average of 39.7 million 100 bp reads per sample, all with a Pfred score at or above 20. The high-quality reads were aligned with the *Arabidopsis* TAIR10 genome with an average mapping efficiency of 97.8% uniquely mapped reads (Supplemental Table S4).

2.2. Constitutive Phytohormone and Gene Expression Levels

Constitutively, gene expression was highly conserved between the two genotypes (~20,469 genes) (Figure 1A); less than 1% were differentially expressed between WT and *lox2* at any time point. In WT plants compared with *lox2* mutants, there was an increase in specialized metabolism, glutathione metabolism and phenylpropanoid biosynthesis (Figure 1B,C). However, some pathogen resistance-related genes had higher expression levels in *lox2* plants compared with WT plants, which may reflect the increased SA levels in these plants (Figure 2). These transcripts included genes that encode enzymes in SA biosynthesis (i.e., AtICS1, AtCM3, AtAIM1 [37]) and SA-responsive genes (i.e., *AtPR1*, *AtNIMIN1*, *AtNIMIN2*, *AtGRXS13* [38]). In contrast, constitutive levels of the jasmonate phytohormone OPDA and JA were higher in WT plants compared with the *lox2* mutant (Figure 3A,B).

A.

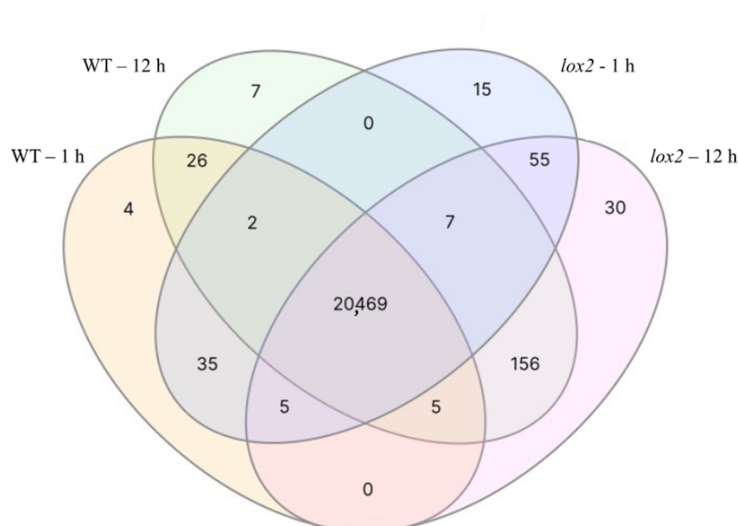
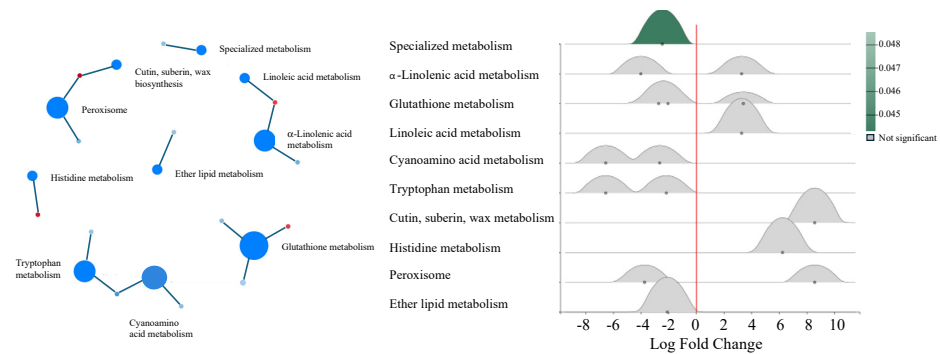


Figure 1. Cont.

B. WT vs *lox2*: Constitutive 1 h



C. WT vs *lox2*: Constitutive 12 h

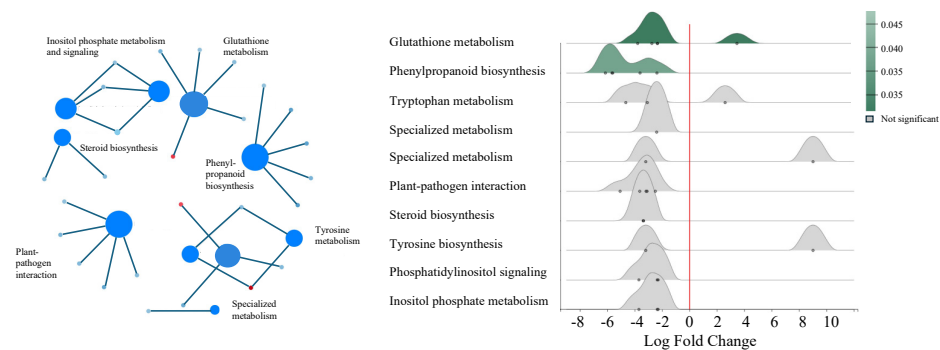
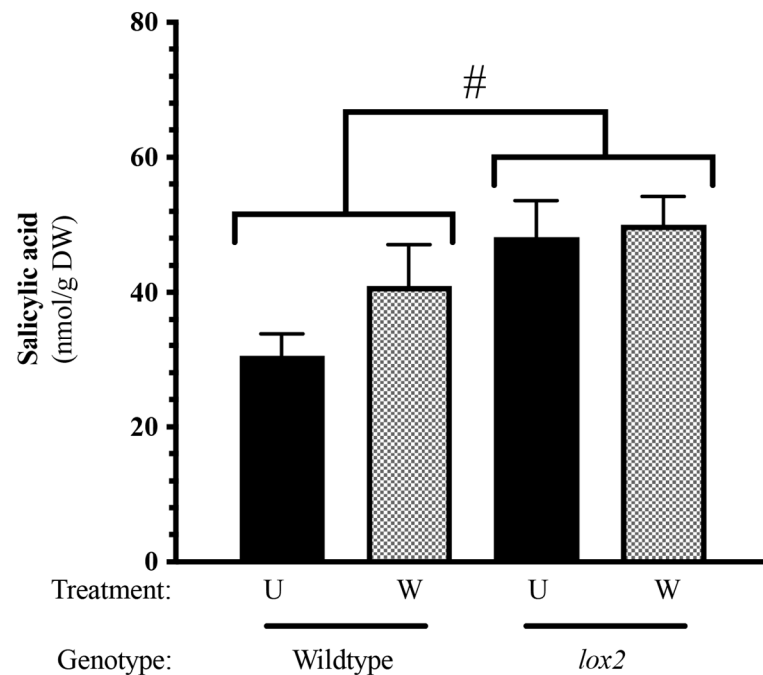


Figure 1. Foliar constitutive gene expression. (A): Venn diagram of constitutive genes differentially expressed between wildtype (WT) and *lox2 Arabidopsis thaliana* plants at two time points (1 and 12 h). Differentially expressed genes between the different treatments and times were determined by DESeq2 (p -value (p_{adj}) ≤ 0.05 and \log_2 fold change ≥ 2 or ≤ -2). (B): Gene set enrichment analysis (GSEA) and ridgeline plot highlighting constitutive metabolic pathways differentially expressed between WT and *lox2* plants at 1 h. (C): GSEA and ridgeline plot highlighting constitutive metabolic pathways differentially expressed between WT and *lox2* plants at 12 h. The ridgeline plot visualizes the distribution of differential enrichment categories identified by GSEA. Significantly differentially expressed pathways in ridgeline plots are indicated in green.

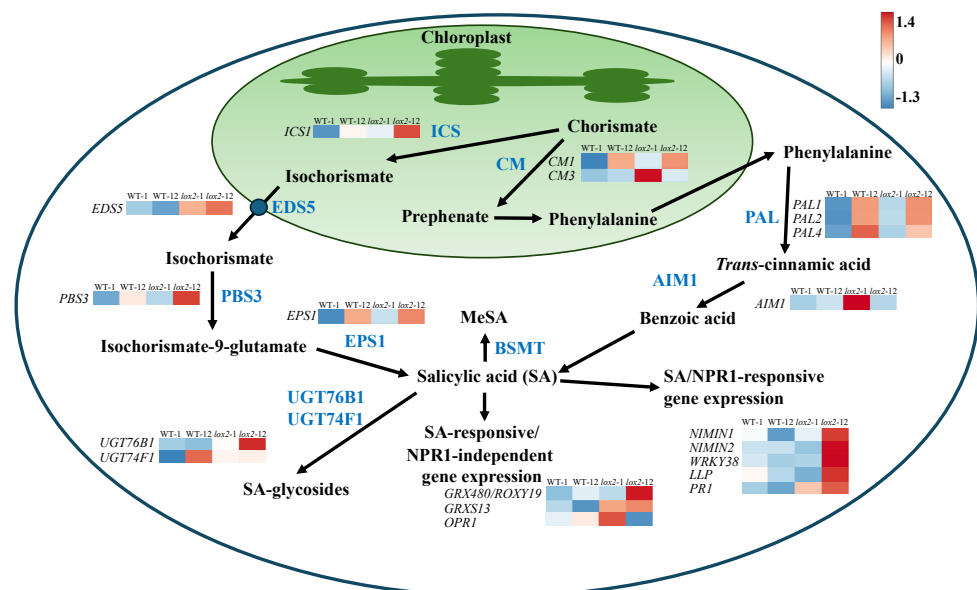
2.3. *Arabidopsis* Responses to Foliar Damage

After wounding, the levels of JA and JA-Ile rose in damaged rosette leaves in both or only WT genotypes, respectively (Figure 3B,C). As expected, levels of these phytohormones were ~ 7.5 times higher in WT than the *lox2* mutant. Jasmonate signaling is dynamic with the early expression of genes encoding biosynthetic enzymes and positive regulators (Figure 3D) [39–41]. In addition, the jasmonate burst is tempered either by catabolizing jasmonates to a less active form or by the activity of JAZ proteins that bind to and repress MYC2/3/4 transcription factors [42,43].

In WT plants, 324 genes were differentially expressed in response to wounding, with 252, 58 and 14 expressed early, late or at both time points, respectively. At 1 h after wounding, a strong increase in the expression of transcripts that encode proteins involved in α -linolenic and linoleic acid biosynthesis, phytohormone and MAPK signaling, terpenoid biosynthesis and wound healing (cutin, suberin and wax biosynthesis) as well as redox metabolism (glutathione metabolism) was observed (Figure 4A,B,E,F). Though most of the processes observed 1 h post-damage were also observed later, there was also an increase in primary metabolic pathways 12 h after wounding. In contrast, though the same general pathways were upregulated in the *lox2* mutant (Figure 4C,D), fewer genes were strongly expressed (Figure 4G,H).

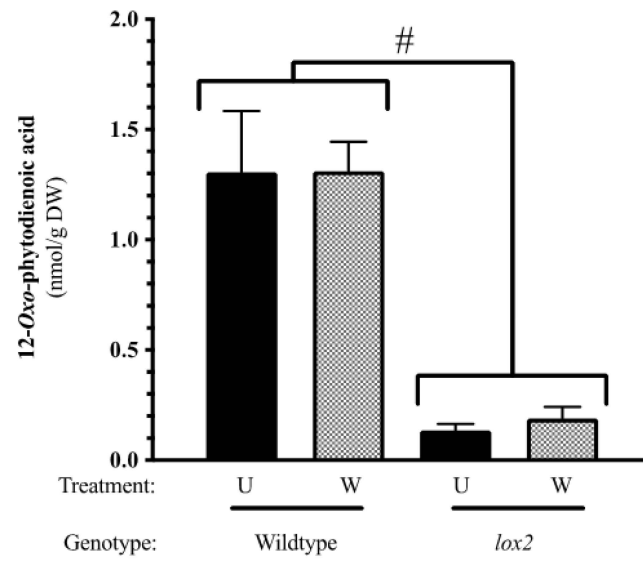


(A) Salicylic acid levels

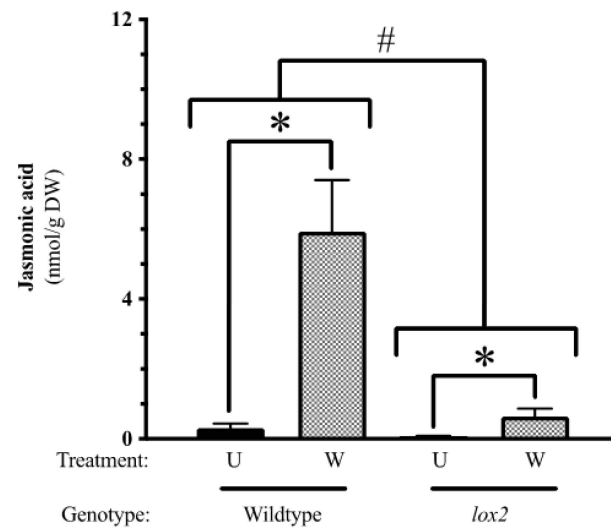


(B) Salicylic acid biosynthesis and signaling

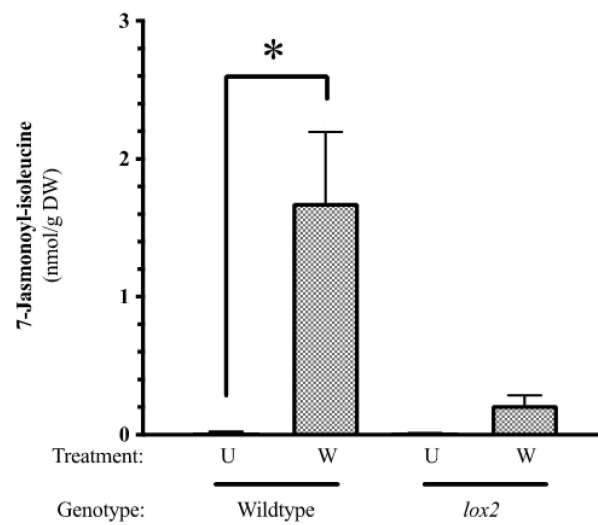
Figure 2. Foliar salicylic acid (SA) levels and SA-related gene expression. Four-week-old *Arabidopsis thaliana* wildtype (WT) or *lox2* plants were left undamaged (U) or wounded (W) with a hole punch on each fully expanded rosette leaf and harvested 1 or 12 h post-damage. (A): Foliar salicylic acid (SA) levels. (B): Constitutive expression of genes involved in SA biosynthesis and SA-responsive gene expression. Phytohormone levels are represented by the mean \pm SE. Differences in phytohormone levels were determined by two-factor analysis of variance (2-factor ANOVA) (factors: genotype, treatment) followed by Tukey HSD (Supplemental Table S2). A hashtag (#) indicates genotype differences. Heatmaps visualize constitutive gene expression (wildtype—1 h (WT-1), wildtype—12 h (WT-12), *lox2*—1 h (*lox2*-1), *lox2*—12 h (*lox2*-12)). Genes: *ICS1/SID2/EDS16* (At1g74710), *EDS5* (At4g39030), *PBS3* (At5g13320), *EPS1* (At5g67160), *CM1* (At3g29200), *CM3* (At1g69370), *PAL1* (At2g37040), *PAL2* (At3g53260), *PAL4* (At3g10340), *AIM1* (At4g29010), *NIMIN1* (At1g02450), *NIMIN2* (At3g25882), *WRKY38* (At5g22570), *LLP* (At5g03350), *PR1* (At2g14610), *GRX480/ROXY19* (At1g28480), *GRXS13* (At1g03850), *OPR1* (At1g76680), *UGT74F1* (At2g43840), *UGT76B1* (At3g11340), *BSMT1* (At3g11480).



(A) 12-Oxo-phytyldienoic acid levels

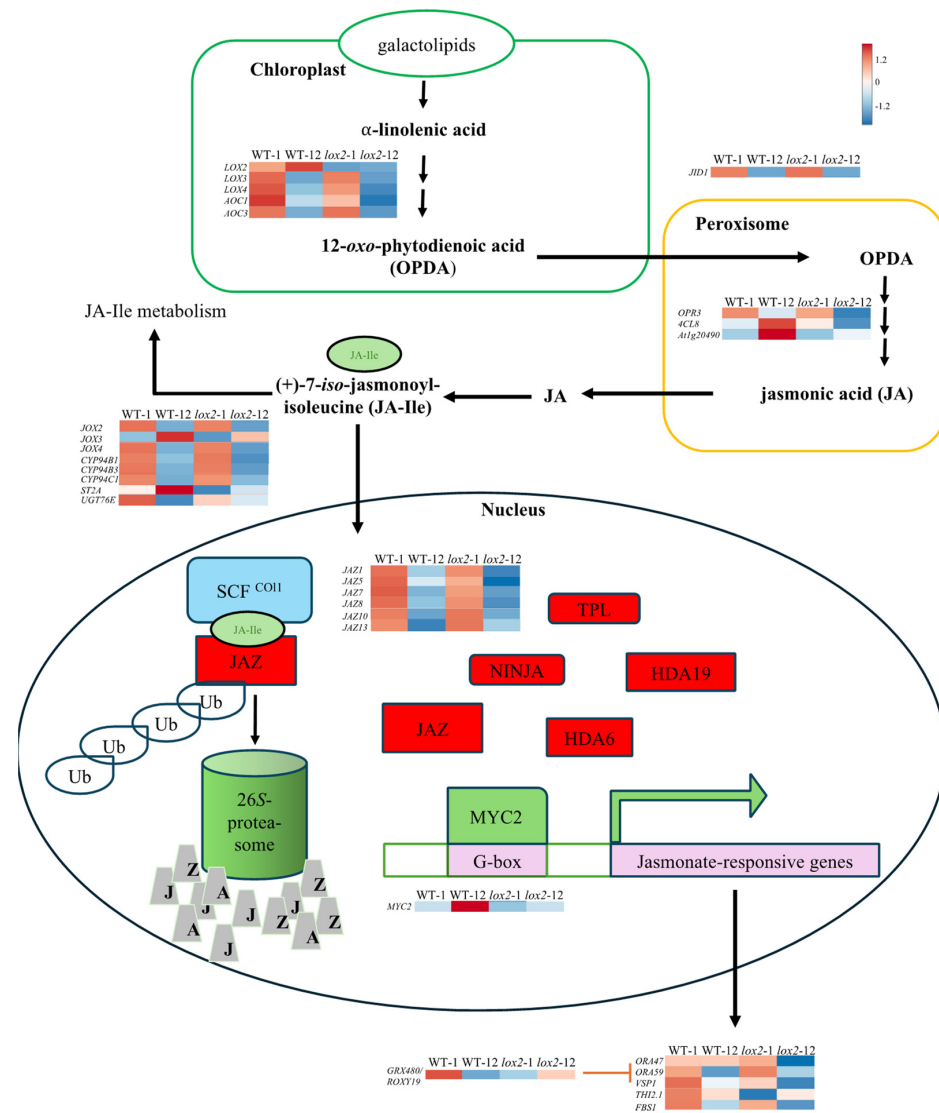


(B) Jasmonic acid levels



(C) 7-Jasmonoyl-isoleucine levels

Figure 3. Cont.



(D) Jasmonate biosynthesis and signaling

Figure 3. Foliar jasmonate levels and jasmonate-related gene expression. Four-week-old *Arabidopsis thaliana* wildtype (WT) or *lox2* plants were left undamaged (U) or wounded (W) with a hole punch on each fully expanded rosette leaf and harvested 1 or 12 h post-damage. Jasmonate levels 1 h after wounding: (A): 12-oxo-phytodienoic acid (OPDA), (B): jasmonic acid and (C): 7-jasmonyl-isoleucine (JA-Ile). (D): Foliar wound-induced jasmonate-related gene expression (1 and 12 h). Phytohormone levels are represented by the mean ± SE. Differences in phytohormone levels were determined by two-factor analysis of variance (2-factor ANOVA) (Factors: genotype, treatment) followed by Tukey HSD (Supplemental Table S2). An asterisk (*) indicates wound-induced phytohormone levels and a hashtag (#) represents genotype differences. Wound-induced genes were determined by DESeq2 (p -value (padj) ≤ 0.05 and \log_2 fold change ≥ 2 or ≤ −2). Heatmaps visualize wound-induced gene expression (wildtype—1 h (WT-1), wildtype—12 h (WT-12), *lox2*—1 h (*lox2*-1), *lox2*—12 h (*lox2*-12)). Genes: *LOX2* (At3g45140), *LOX3* (At1g17420), *LOX4* (At1g72520), *AOC1* (At3g25760), *AOC3* (At3g25780), *OPR3* (At2g06050), *OPCL1* (At1g20510), *At1g20490*, *FBS1* (At1g61340), *MYC2* (At1g32640), *JAZ1* (At1g19180), *JAZ5* (At1g17380), *JAZ7* (At2g34600), *JAZ8* (At1g30135), *JAZ10* (At5g13220), *JAZ13* (At3g22275), *JOX2* (At5g05600), *JOX3* (At3g55970), *JOX4* (At2638240), *CYP94B1* (At5g63450), *CYP94B3* (At3g48520), *CYP94C1* (At2g27690), *ST2A* (At5g07010), *JID1* (At1g06620), *ORA47* (At1g74930), *ORA59* (At1g6160), *VSP1* (At5g24780), *THI2.1* (At1g72260), *GRX480/ROXY19* (At1g28480).

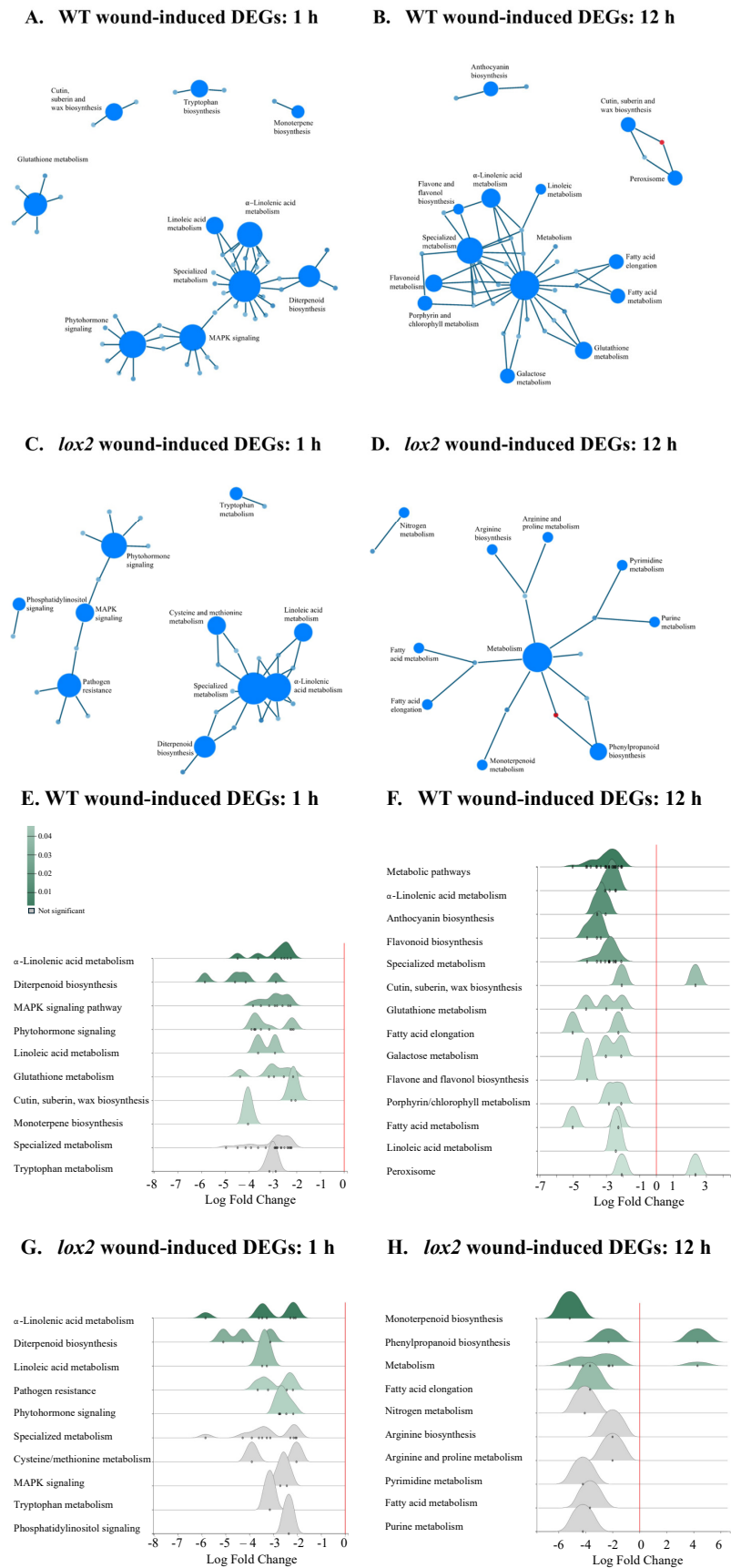


Figure 4. Wound-induced foliar gene expression. Four-week-old *Arabidopsis thaliana* wildtype (WT) or *lox2* plants were wounded with a hole punch on each fully expanded rosette leaf and harvested at 1 and 12 h. Gene set enrichment analyses (GSEA) and ridgeline plots of WT (1 h) (A,E), WT (12 h)

(B,F), *lox2* (1 h) (C,G) and *lox2* (12 h) (D,H). Wound-induced differentially expressed genes (DEGs) were determined by DESeq2 (p -value (padj) ≤ 0.05 and \log_2 fold change ≥ 2 or ≤ -2). The ridgeline plot visualizes the distribution of differential enrichment categories identified by GSEA. Significantly differentially expressed pathways in ridgeline plots are indicated in green.

In general, WT and *lox2* plants showed similar wound-induced responses (Figure 5A,D). One hour post-damage, out of the 249 wound-induced genes observed in WT plants, 81% were also induced in damaged *lox2* (Figure 5A,B). A stronger difference in wound-induced gene expression between WT and *lox2* plants was observed 12 h after wounding (Figure 5D,E). At this time point, only 76 wound-induced genes were identified in WT and shared 31% gene expression with damaged *lox2*.

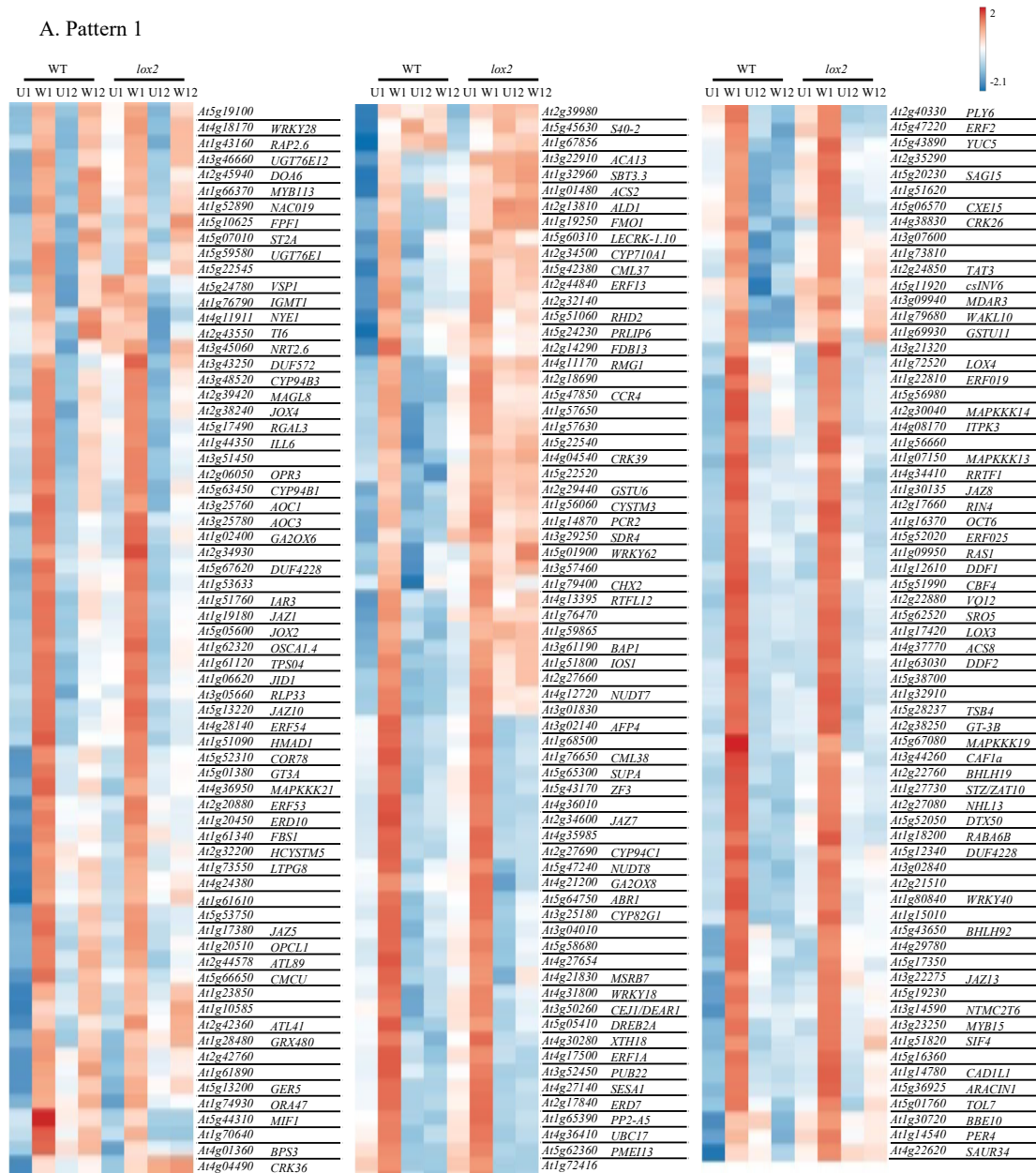
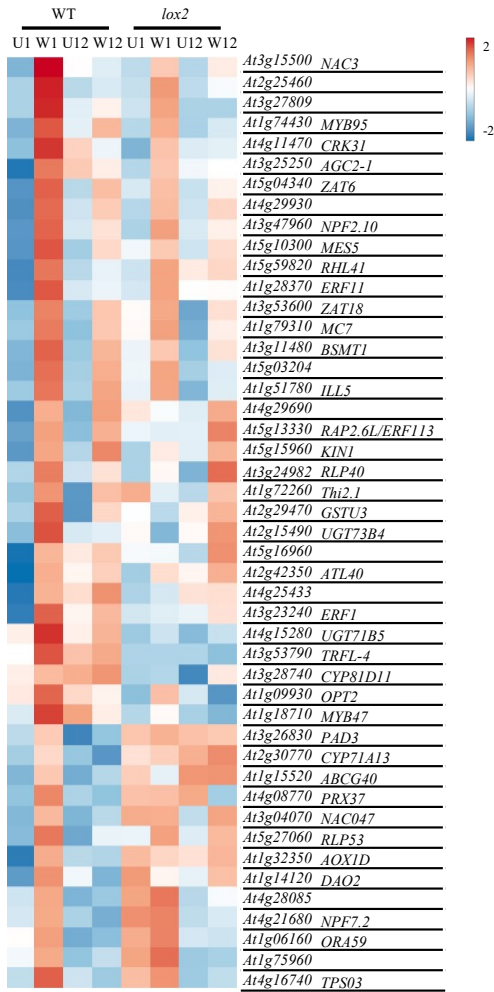
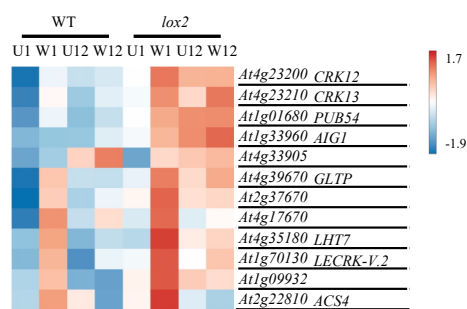


Figure 5. Cont.

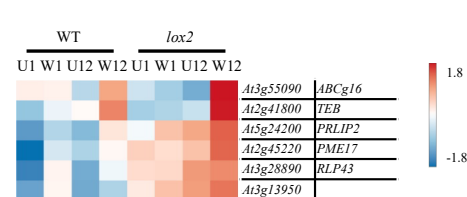
B. Pattern 2



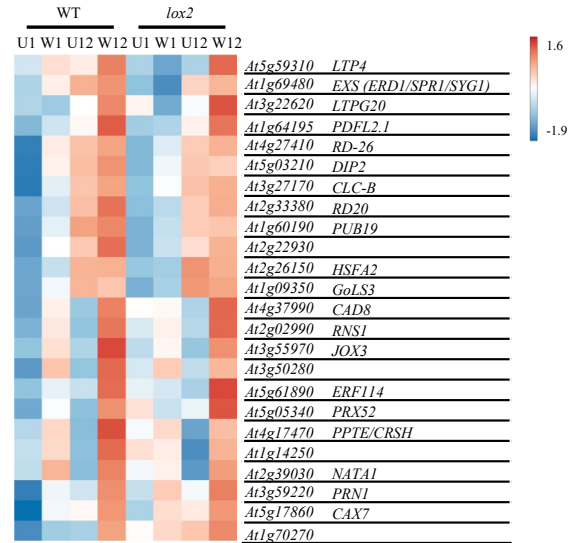
C. Pattern 3



F. Pattern 6



D. Pattern 4



E. Pattern 5

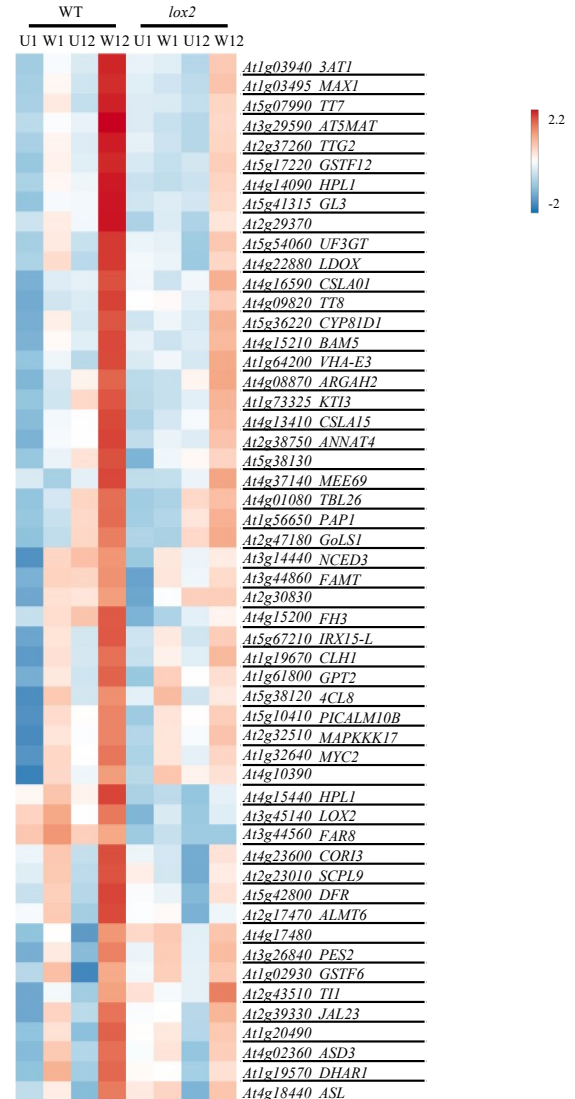


Figure 5. Wound-induced foliar gene expression: Patterns. Four-week-old *Arabidopsis thaliana* wildtype (WT) or *lox2* plants were wounded with a hole punch on each fully expanded rosette leaf

and harvested at 1 and 12 h. Wound-induced genes fell into six general expression patterns visualized by heatmaps. Early gene expression (peak at 1 h): (A) general-both genotypes, (B) WT and (C) *lox2*. Later gene expression (peak 12 h): (D) general-both genotypes, (E) WT and (F) *lox2*. Wound-induced genes were determined by DESeq2 (p -value (padj) ≤ 0.05 and \log_2 fold change ≥ 2 or ≤ -2) (Supplemental Table S5). Heatmaps visualize gene expression (undamaged-U, wound-W, 1 h-1, 12 h-12).

Based on this, wound-induced gene expression patterns were divided into six distinct groups as follows: Pattern 1—general early (1 h) wound-induced gene expression (Figure 5A), Pattern 2—early (1 h) wound-induced gene expression with higher expression in WT plants (Figure 5B), Pattern 3—early (1 h) wound-induced gene expression with higher expression in *lox2* plants (Figure 5C), Pattern 4—general late (12 h) wound-induced gene expression (Figure 5D), Pattern 5—late (12 h) wound-induced gene expression with higher expression in WT plants (Figure 5E) and Pattern 6—late (12 h) wound-induced gene expression with higher expression in *lox2* plants (Figure 5F).

2.4. Pattern 1: General Early Wound-Induced Gene Expression

In this group, wound-induced gene expression is higher at 1 h and typically returned to near-basal levels at 12 h in both genotypes (Figure 5A, Supplemental Table S5A). One hour post-damage, the expression of genes encoding proteins involved in jasmonate biosynthesis and signaling were strongly upregulated in both genotypes (i.e., *AtLOX3*, *AtLOX4*, *AtLOX6*, *AtAOC1*, *AtAOC3*, *AtOPR3*, *AtOPCL1* and *AtORA47* [39–41]) (Figure 3D). In addition, genes encoding proteins involved in jasmonate anabolism (i.e., *AtJOX2*, *AtJOX4*, *AtCYP94B1*, *AtCYP94B3*, *AtILL6* and *AtJID1* [44–48]) and JAZ proteins (*AtJAZ1*, *AtJAZ2*, *AtJAZ5*, *AtJAZ7*, *AtJAZ8*, *AtJAZ10*, *AtJAZ13* [42,43]) were also induced.

In line with this, jasmonate-responsive genes were among the early responding genes including those that encode enzymes in volatile biosynthesis (i.e., *AtTPS04/GES*, *AtCYP82G1* [49,50]), enzymes involved in sealing damaged tissue (i.e., *AtPP2-A5* [51]), transcription factors (i.e., *AtRRTF1*, *AtWRKY40*, *AtRAP2.6* [52–56]) and proteins involved in plant defense against pathogens or insects (i.e., *AtTI6*, *AtMAPKKK21* [57,58]).

Gene expression associated with other phytohormones and their signaling pathways that may be involved in crosstalk were also observed. Wound-induced expression of *AtGA2OX6* and *AtGA2OX8*, encoding enzymes that oxidize gibberellins lowering their availability [59], as well as the negative growth regulator DELLA protein *AtRGAL3* [60,61], may reflect the shift from growth to defense [62]. Even though abscisic acid (ABA) levels were not affected by wounding (Supplemental Figure S1), a number of ABA-related genes were induced 1 h after wounding. The expression of the ABA receptor *AtPYL6* and ABA-responsive genes (i.e., *AtRAS1*, *AtERD7*, *AtOSCA1.4*, *AtERD10*, *AtCOR78* [63–67]) were upregulated early after foliar damage. ABA-related responses help minimize water loss from damaged leaves as well as enhance plant defense responses [68–70]. In response to wounding, synergistic defensive responses between jasmonates and ethylene are often observed [71]; genes encoding ethylene biosynthetic enzymes (i.e., *AtCSP2* and *AtACS8*) and ethylene responses (i.e., *AtERF2* and *AtRAP2.6*) were noted in early wound-induced responses.

LOX2 has been implicated in wound-associated, chloroplastic generation of $^1\text{O}_2$ [34,35]. Comparing transcript expression of 66 $^1\text{O}_2$ -responsive genes in our damaged foliar tissues 1 h post-wounding [72,73], a genotype-difference in wound-induced $^1\text{O}_2$ -responsive transcript expression was not observed (Supplemental Figure S2).

2.5. Pattern 2: Early Wound-Induced Gene Expression in WT Plants

In general, genes in this group were often wound-induced in both WT and *lox2* but showed earlier, higher expression levels in WT plants (Figure 5B, Supplemental Table S5B). These early damage-induced genes include transcriptional regulators of jasmonate responses (i.e., *AtORA59* [74]) as well as jasmonate- and wound/insect-responsive genes (i.e., *AtTHI2.1*, *AtTPS03*, *AtCYP81D11* [75–78]).

2.6. Pattern 3: Early Wound-Induced Gene Expression in *lox2* Plants

Likely reflecting elevated SA levels (Figure 2, Supplemental Table S5C), SA-responsive genes (*AtAIG1*, *AtCRK13* [79,80]) were expressed at higher levels in wounded *lox2* mutants compared with WT plants (Figure 5C).

2.7. Pattern 4: General Late Wound-Induced Gene Expression

Pattern 4 shows wound-induced genes in both genotypes that were more highly expressed 12 h after mechanical damage (Figure 5D, Supplemental Table S5D). Late wound-induced genes in both plant genotypes include *AtPDFL2.1*, *AtNATA1*, *AtRD20*, *AtPRN1*, *AtPPTE/AtCRSH* and *AtRNS1*. Genes encoding enzymes in lignin biosynthesis (i.e., *AtCAD8*, *AtPRX52*) may also contribute to wound-induced lignin deposition (Figure 6) [81,82].

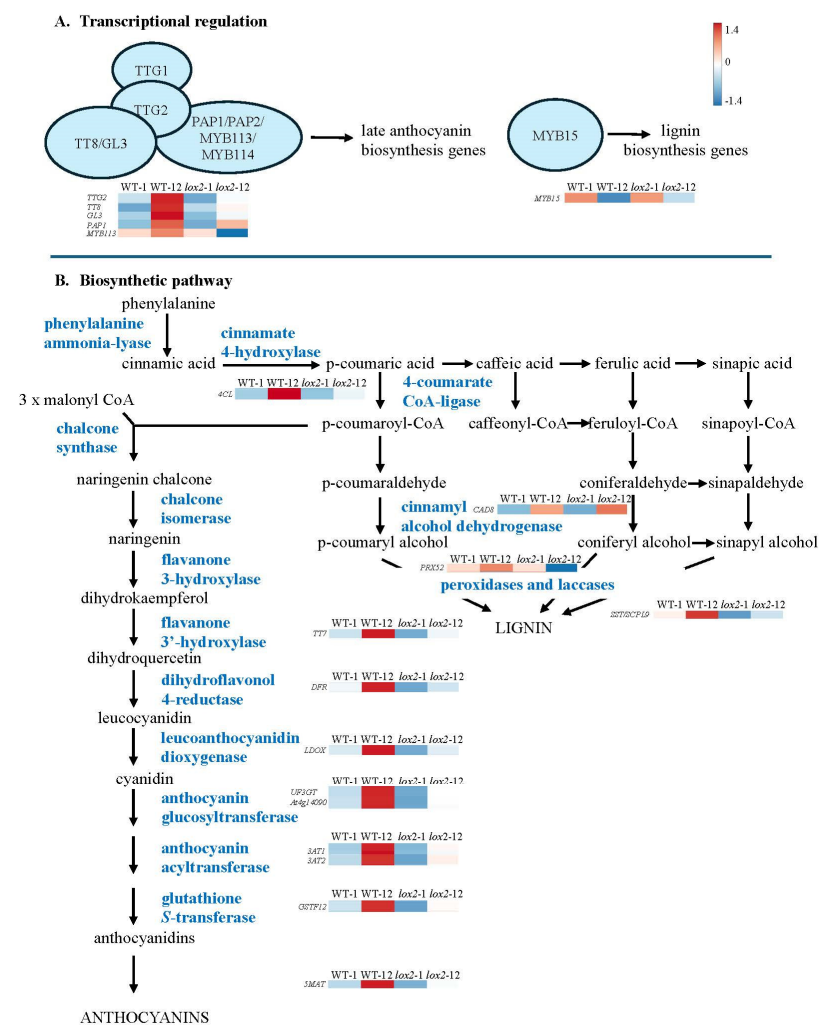


Figure 6. Wound-induced genes involved in polyphenol biosynthesis. Four-week-old *Arabidopsis thaliana* wildtype (WT) or *lox2* plants were wounded with a hole punch on each fully expanded rosette leaf and harvested at 1 or 12 h. (A) Transcriptional regulators and (B) biosynthetic genes. Wound-induced genes were determined by DESeq2 (p -value (padj) ≤ 0.05 and \log_2 fold change ≥ 2 or ≤ -2). Heatmaps visualize wound-induced gene expression (wildtype—1 h (WT-1), wildtype—12 h (WT-12), *lox2*—1 h (*lox2-1*), *lox2*—12 h (*lox2-12*)). Genes: *TTG2* (*At2g37260*), *TT8* (*At4g09820*), *GL3* (*At5g41315*), *PAP1* (*At1g56650*), *MYB113* (*At1g66379*), *4CL* (*At1g20490*), *TT7* (*At5g07990*), *DFR* (*At5g42800*), *LDOX* (*At4g22880*), *UFGT* (*At5g54060*), *At4g14090*, *3AT1* (*At1g03840*), *3AT2* (*At1g03495*), *GSTF12* (*At5g17220*), *5MAT* (*At3g29590*), *MYB15* (*At3g23250*), *CAD8* (*At4g37990*), *PRX52* (*At5g05340*), *SST/SCPL9* (*At2g23010*).

2.8. Pattern 5: Late Wound-Induced Gene Expression in WT Plants

Most late-induced genes showed higher expression in WT plants compared with *lox2* plants 12 h post-damage (Figure 5E, Supplemental Table S5E). This likely reflects the expression of genes encoding enzymes in jasmonate biosynthesis (*AtLOX2*, *At4CL8*) and signaling (*AtMYC2*) that were more highly expressed in wounded WT compared with *lox2* plants [4]. Jasmonate-responsive genes involved in plant resistance to insect herbivory, such as *AtHPL/AtCYP74B2*, which encodes an enzyme involved in volatile biosynthesis [83], *AtCLH1*, *AtKTI3*, *AtTI1*, *AtARGAH2* and *AtMAPKKK17*, reflect this pattern [58,84–86]. Genes involved in antioxidant pathways are upregulated in wounded WT plants, including those that encode proteins involved in the ascorbate/glutathione cycle (i.e., *AtDHAR1* [87]) and anthocyanin biosynthesis (i.e., *AtPAP1*, *AtTT8*, *AtGL3*, *AtTTG2*, *At4CL*, *AtTT7*, *AtDFR*, *AtLDOX*, *AtUF3GT*, *At1g14090*, *At3AT1*, *At3AT2*, *AtGSTF12*, *At5MAT* [88–90]) (Figure 6). Of note, *AtTTG1* and *AtGL3* also regulate trichome development [91].

2.9. Pattern 6: Late Wound-Induced Gene Expression in *lox2* Plants

Only a few genes showed *lox2*-specific late wound-induced expression (Figure 5F, Supplemental Table S5F). Expression of the SA-responsive gene *AtPRLIP2* was observed in wounded *lox2* mutants [92,93].

2.10. Glucosinolates

Constitutively or 12 h post-wounding, the foliar GSL profile did not differ between the two genotypes, reflecting the gene expression profile of GSL biosynthetic enzymes (Figure 7A). However, genes encoding GSL transcriptional regulators and biosynthetic enzymes show a strong diurnal cycle with stronger expression in the light phase, particularly for genes involved in aliphatic GSL biosynthesis (Figure 7B). Genes encoding indole GSL methyltransferase1 (*AtGMT1*), the GSL transporter *AtNPF2.10* and lectin *JAL23* (a polymerization factor and putative activator of the myrosinase *PYK10* [94]) showed strong wound-induction in WT plants.

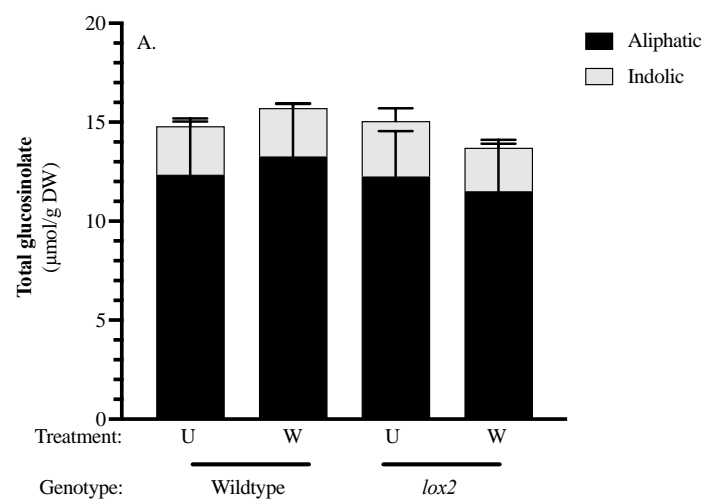
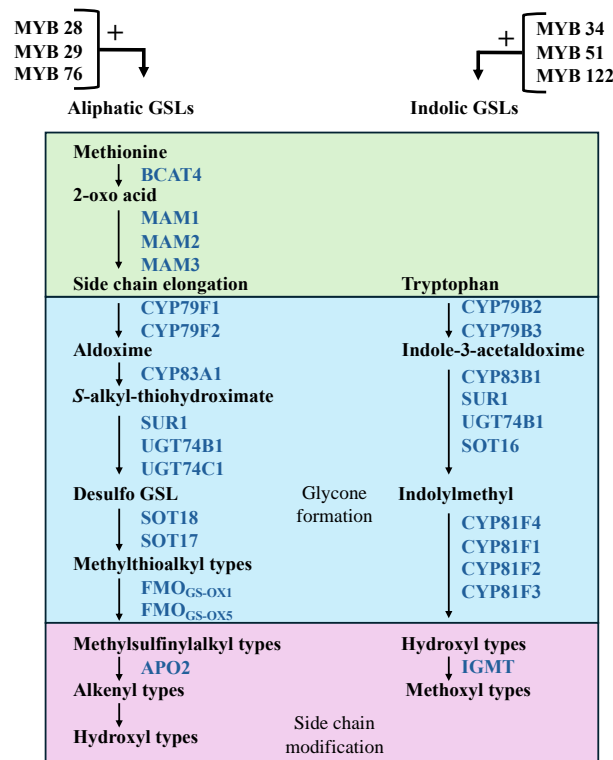
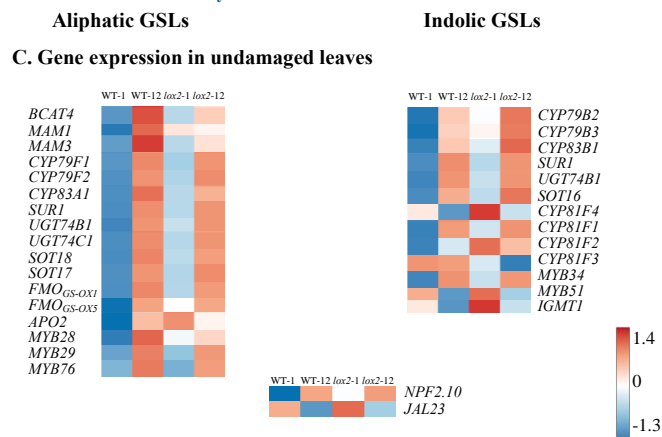


Figure 7. Cont.

B. Glucosinolate biosynthetic pathway



NPF2.10: GSL/H⁺ transporter
 JAL23: polymerizer/activator lectins of PYK10 myrosinases



D. Gene expression in mechanically wounded leaves (12 h)

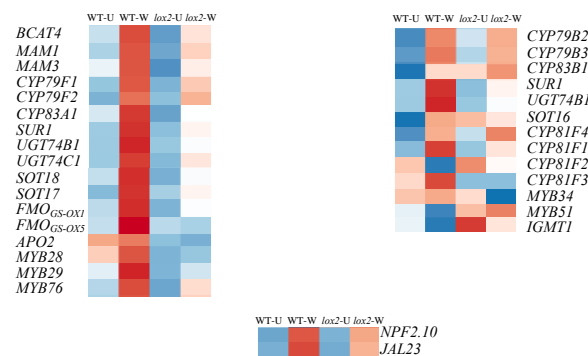


Figure 7. Foliar glucosinolate (GSL) levels and expression of GSL biosynthesis genes. Four-week-old *Arabidopsis thaliana* wildtype (WT) or *lox2* plants were wounded with a punch on each fully

expanded rosette leaf and harvested at 1 and 12 h. (A) Foliar aliphatic and indolic GSL levels in undamaged (U) and wounded (W) WT and *lox2* plants taken 12 h after mechanical damage. (B) GSL pathway illustrating transcriptional activators, biosynthetic enzymes and other GSL-related proteins. Gene expression in (C) undamaged and (D) mechanically damaged arabidopsis rosettes. Glucosinolate levels are represented by the mean \pm SE. Differences in GSL levels were determined by a two-factor analysis of variance (2-factor ANOVA) (factors: genotype (WT or *lox2*), treatment) followed by Tukey HSD (Supplemental Table S3). Heatmaps visualize gene expression (for C: wildtype—1 h (WT-1), wildtype—12 h (WT-12), *lox2*—1 h (*lox2*-1), *lox2*—12 h (*lox2*-12); for D: wildtype undamaged—WT-U, wildtype wounded—WT-W, *lox2* undamaged—*lox2*-U, *lox2* wounded—*lox2*-W)). Genes: *BCAT4* (At3g19710), *MAM1* (At5g23010), *MAM3* (At5g23020), *CYP79F1* (At1g16410), *CYP79F2* (At1g16400), *CYP83A1* (At4g13770), *SUR1* (At2g20610), *UGT74B1* (At1g24100), *UGT14C1* (At2g31790), *SOT18* (At1g74090), *SOT17* (At1g18590), *FMO_{GS-OX1}* (At1g65860), *FMO_{GS-OX5}* (At1g12140), *APO2* (At5g57930), *MYB28* (At5g61420), *MYB29* (At5g07690), *MYB76* (At5g07700), *NPF2.10* (At3g47960), *JAL23* (At2g39330), *CYP79B2* (At4g39950), *CYP79B3* (At2g22330), *CYP83B1* (At4g31500), *UGT74B1* (At1g24100), *SOT16* (At1g74100), *CYP81F4* (At4g37410), *CYP81F1* (At4g37430), *CYP81F2* (At5g57220), *CYP81F3* (At4g37400), *IGMT1* (At1g21100), *MYB34* (At5g60890), *MYB51* (At1g18570).

3. Discussion

Our results highlight the transcriptional dynamics of wound-induced jasmonate biosynthesis and the importance of AtLOX2 in sustained jasmonate signaling leading to plant resistance against insect herbivores.

3.1. The Dynamic Jasmonate Burst

Early wound-induced genes in both genotypes include enzymes in the jasmonate biosynthetic pathway (i.e., AtLOX3, AtLOX4, AtAOC1, AtAOC3, AtOPR3, AtOPCL1 [4]) and transcriptional regulators (i.e. AtORA47) (Pattern 1, Figure 5A). ORA47 coordinates the expression of genes that encode jasmonate and ABA biosynthetic enzymes as well as in the general jasmonate-responsive stress network [41,95,96]. The expression of later genes that encode jasmonate biosynthetic enzymes (i.e., AtLOX2, At4CL8, At1g20490 (putative) [4,97]) were generally higher in WT compared with *lox2* plants (Pattern 5, Figure 5E). This was reflected in the expression of jasmonate-responsive gene expression, particularly in late wound-induced genes (Figure 5).

The wound-induced jasmonate burst is dynamic, and the initial strong jasmonate wave is dampened over time. Indeed, early wound-induced transcriptional expression included genes encoding proteins that attenuate the jasmonate-mediated signaling response, in particular, enzymes that metabolize jasmonates to their inactive form (i.e., AtST2A, AtJOX2, AtJOX4, AtCYP94B1, AtCYP94B3, AtILL6, AtJID1) and JAZ proteins (i.e., AtJAZ1, AtJAZ5, AtJAZ7, AtJAZ8, AtJAZ10, AtJAZ13) (Pattern 1, Figure 5A). JAZ proteins are negative regulators that bind to jasmonate signaling MYC2, MYC3 and MYC4 transcription factors [42,43]. Early wound-induced JAZ transcripts encode AtJAZ1, AtAtJAZ5, AtJAZ8, AtJAZ10 and AtJAZ13, which interact with AtMYC2 or AtMYC3, as well as AtJAZ7, which interacts with AtMYC2 [98–100].

In addition, early wound-induced genes include a number of enzymes that convert jasmonates into an potentially inactive forms (Pattern 1, Figure 5A). 2-oxo-glutarate-dependent dioxygenase genes *jasmonate-induced oxidase2* (AtJOX2) and AtJOX4 as well as the aminohydrolase AtILL6 are expressed early after wounding, while AtJOX3 is expressed later (Figure 3); these genes encode enzymes that hydroxylate JA to a biologically inactive form [45–47]. Subsequently, the hydroxylated JA can be further metabolized by sulfotransferase 2A (ST2A) to the sulfated form [101]. Furthermore, the early wound-induced cytochrome P₄₅₀ genes encoding AtCYP94B1, AtCYP94C1 and AtCYP94B3 potentially work in sequence to catalyze the formation of 12-OH-JA-Ile and 12-COOH-JA-Ile, respectively [44,102–104]. JID1 is a cytosolic enzyme thought to be involved in OPDA anabolism [48].

Often working synergistically, ethylene and jasmonate signaling leads to increased plant resistance [105]. Early genes encoding enzymes in ethylene biosynthesis, *AtACS2*, *AtACS8* and *AtACS4*, as well as the transcription factors *AtRAP2.6*, *AtERF2* and *AtERF114*, were wound-induced in WT or both genotypes 1 h post-damage (Figure 5A,C).

In comparison, SA and jasmonates often have an antagonistic relationship that acts to shape the plant defense response [106]. In general, the *lox2* mutant expressed higher constitutive expression of genes involved in SA biosynthesis (i.e., *AtICS*, *AtEDS5*, *AtPBS3*, *AtCM3*, *AtAIMI* [37,107]) that translated into higher SA levels and SA-responsive gene expression (i.e., *AtGRX480/AtROXY19*, *AtCRXS13*, *AtOPR1*, *AtNIMIN1*, *AtNIMIN2*, *AtWRKY38*, *AtLLP*, *AtPR1*) (Figure 2). Of these, *AtNIMIN1*, *AtNIMIN2* and *AtWRKY38*, which encode negative regulators of basal immunity [108–110], were expressed in the light (9 am), which may reflect the diurnal rhythm of SA, which is lower in the morning [111]. In wounded plants, SA-responsive *AtCRK13*, *AtAIG1* and *AtPRLIP2* were more highly expressed in *lox2* compared with WT plants (Pattern 3, Figure 5C; Pattern 6, Figure 5F) [79,80,92,93].

3.2. Plant Resistance against Insect Herbivory

3.2.1. Response to Egg Deposition

In some species, plants respond to insect eggs by eliciting an SA-dependent “hypersensitive-like response” that results in necrotrophic tissue forming under the eggs, often leading to egg desiccation and plant resistance [112]. Treatment of leaves by spider mite egg extract resulted in the induction of genes encoding enzymes in the jasmonate biosynthesis and signaling pathway (i.e., *AtAOC1*, *AtAOC3*, *AtLOX2*, *AtMYC2*, *AtJAZ9*, *AtST2A*, *AtJOX2*, *AtJOX3*, *AtJOX4*, *AtILL6*, *AtCYP82G1*, *AtMDHAR*, *AtFAMT*, *AtNATA1*, *AtZAT10/STZ*, *AtBSMT1*, *RNS1 At3g23350* and *AtCORI3*), which were also seen in our study (Figures 3D and 5) [113].

3.2.2. Signal Transduction

In this and other studies, *AtMAPKKK17*, induced late in response to wounding in WT plants (Pattern 5, Figure 5E), activates the MKK3-MPK1/2/7 module [114,115]. In plants challenged with the two-spotted spider mite, *Tetranychus urtica*, plants with higher constitutive *AtMAPKKK17* expression had higher resistance against mite herbivory, exhibiting less leaf damage with mites having lower fecundity [58]. *AtMAPKKK21* is expressed early after wounding in both genotypes (Pattern 1, Figure 5A). In contrast to *MAPKKK17*, this kinase was found to be a negative regulator of plant resistance to mites [58].

3.2.3. Physical Defense

Foliar trichomes create a mechanical defense against insect herbivores and, as well, may be a site for the production of chemical defenses [116]. Even though arabidopsis trichomes are non-glandular, volatile organic compounds as well as aliphatic and indolic GSLs may be biosynthesized in these cells [21,50,117]. In addition, arabidopsis trichomes may serve as mechanosensors, possibly leading to specialized metabolite production when triggered [118,119]. *AtGL3*, a late wound-induced gene that shows higher stress-associated expression in WT compared with *lox2* plants (Pattern 5, Figure 5E), encodes a bHLH transcription factor that regulates trichome initiation as well as anthocyanin biosynthesis [120,121]. Constitutively, this transcription factor interacts with JAZ proteins, specifically, *JAZ1*, *JAZ2*, *JAZ8* and *JAZ11*, leading to its repression [122]. In response to wounding, the resultant degradation of JAZ proteins coupled to increased *AtGL3* expression supports observations of a wound-associated increase in arabidopsis foliar trichomes [123].

3.2.4. Chemical Defense

GSLs and flavonoids are important defensive compounds in the Brassicaceae [18,124,125]. A wound-induced difference in foliar GSL levels was not observed (Figure 7). However, in both genotypes, a strong expression of GSL biosynthetic genes was observed late after wounding, which corresponds to the light phase in our experiment. This supports previous observations of a possible role of circadian rhythms in foliar GSL biosynthesis [21].

In contrast, a genotype difference in wound-induced genes associated with flavonoid biosynthesis was identified in this study, with genes expressed more highly in WT plants (Pattern 5, Figure 6). Flavonoids can act as feeding or oviposition deterrents or toxins against insect herbivores [124,125]. Even though *AtRNS1*, a jasmonate-independent, wound-induced gene that encodes a ribonuclease that is a negative regulator of anthocyanin biosynthesis [126], is expressed in both genotypes (Pattern 4, Figure 5D), the late wound-induced expression of genes that encode transcriptional regulators or flavonoid biosynthetic enzymes was observed in WT plants (Pattern 5, Figure 5E). Thus, particularly in WT plants, there is a strong upregulation of genes involved in flavonoid biosynthesis, particularly anthocyanins, that may act as antioxidants or be involved in plant resistance against insect herbivory [125,127].

3.2.5. Indirect Chemical Defense

Wounding of arabidopsis leaves results in the biosynthesis and release of volatile organic compounds (VOCs) that are involved in numerous ecological roles, including intra-plant stress signaling and tritrophic interactions, such as attracting parasitoids or predators of the herbivore [128,129]. From the diterpenoid precursor geranylgeranyl diphosphate, *AtTPS04*, which is expressed in arabidopsis non-glandular trichomes [50], catalyzes the production of (E,E)-geranylgeranyl acrylate, which is converted by *AtCYP82G1* into volatile 4,8,12-trimethyltrideca-1,3,7,11-tetraene (TMTT) [49], an important attractant in tritrophic interactions for beneficial parasitoid and predatory arthropods [130]. *AtTPS04* is induced in response to herbivory by caterpillars of the specialist diamond backmoth, *Plutella xylostella*, or the generalist African cotton leafworm, *Spodoptera littoralis* [131–134]. In our study, both *AtTPS04* and *AtCYP82G1* show early wound-induced gene expression (Pattern 1, Figure 5A). *AtCYP82G1* is also induced in response to the treatment of arabidopsis leaves with spider mite egg extract [113].

The expression of *AtTPS03* and *AtCYP81D11* is predominant in wounded WT plants (Pattern 2, Figure 5B). *AtTPS03* encodes a terpene synthase that produces (E,E)- α -farnesene, an important component in highly attractive volatile blends attractive to parasitic wasps such as *Microplitis croceipes*, *Apanteles taragamae*, *Anaphes iole* and *Gonatocerus ashmeadi*, as well as acting as a deterrent to soybean cyst nematodes [135–139]. *AtCYP81D11* also contributes to the volatile profile responsible for the attraction of parasitoid wasps, such as *Cotesia plutellae*, to wounded plants [140].

AtHPL had higher late wound-induced expression in WT compared with *lox2* plants (Pattern 5, Figure 5E). This jasmonate-responsive gene is also induced in response to herbivory by *P. rapae* or *S. littoralis* caterpillars [141]. Cytosolic *AtHPL* competes with the jasmonate biosynthetic pathway for 13-hydroperoxide precursors to generate alkenals, which are converted into C6 volatiles [83]. The *AtHPL* in the arabidopsis Col-0 ecotype (which was also used in this study) has a deletion resulting in a truncated protein that is unable to use 13-hydroperoxide linolenic acid as a precursor but uses 13-hydroperoxide linoleic acid to produce hexenals [142].

AtBSMT1 was also more highly wound-induced in WT plants (Pattern 2, Figure 5B). This methyltransferase, involved in volatile methyl salicylate biosynthesis, is induced in response to *P. rapae* and *Pieris brassicae* herbivory [143,144]. The resultant methyl salicylate is an attractant for female parasitic *Diadegma semiclausum* wasps and also deters oviposition by female *P. brassicae* butterflies, thus decreasing herbivore damage [144,145].

In addition to the role that these VOCs play in attracting natural enemies of the herbivore [146], these volatiles can also act on the plant itself, leading to systemic upregulation of plant defense responses [147,148]. Recently, the importance of these volatiles as conspecific signals has been recognized [149]. Thus, volatiles may serve as systemic signals resulting in the induction of plant defense responses.

3.2.6. Interference with Insect Nutrition or Physiology

Obtaining sufficient nitrogen to maintain development and fitness is a key challenge for phytophagous insects [150]. Thus, plants have numerous strategies to interfere with a herbivore's ability to obtain sufficient nitrogen to limit herbivore success.

In herbivorous insects, serine proteinases, such as trypsin and chymotrypsin, initiate protein digestion [151]; However, plants produce inhibitors of these enzymes, known as proteinase inhibitors [152]. Overexpression of a soybean trypsin inhibitor in arabidopsis negatively affected the larval biomass of corn earworm, *Helicoverpa zea*, caterpillars [153]. In our study, we identified the expression of three wound-induced trypsin inhibitors. *AtTI1* is induced early in both genotypes and has previously been found to be induced by aphid attack (Pattern 1, Figure 5A) [154]. *AtKTI3* and *AtTI6* are more highly expressed in WT plants late after wounding (Pattern 5, Figure 5E).

Another late wound-induced gene identified in our transcriptomic study that interferes with nitrogen resources for the insect encodes arginase (AtARGAH2) (Pattern 5, Figure 5E). This enzyme catabolizes nitrogen-rich arginine to produce urea and ornithine. Direct feeding of *Manduca sexta* caterpillars on tomato plants overexpressing arginase resulted in smaller insects, presumably because of the decreased availability of the essential amino acid arginine [86]. However, this may also reflect the potential toxicity of arginase products, where ornithine may be converted by AtNATA1, a late pattern 4 gene (Figure 5D), to N^d-acetylornithine [155]. This derivative negatively affects the fecundity of the green peach aphid, *Myzus persicae*. It is of interest that the pH optimum of plant arginase is alkaline [86], which likely allows it to be most active in its native cellular location, the mitochondrial matrix [156], and also in the alkaline midgut of caterpillars [157]. In addition to these activities, ARGAH2 activity may affect nitric oxide (NO) production [158]. Though this has been shown in the marine green algae *Ostreococcus tauri* [159], in higher plants, NOS-like activity is controversial; however, NO has been proposed to be released from arginine upon its conversion to citrulline [160,161]. Consistent with this, AtARGAH2 knockout plants had increased NO accumulation [158]. Differences in NO, or its more biologically stable form S-nitrosoglutathione (GSNO), can impact protein S-nitrosation and S-glutathionylation status of regulatory proteins involved in plant defense [162–165]. *Manduca sexta* caterpillars grew larger on plants silenced in their ability to produce GSNO. Methyl jasmonate-induced levels of proteinase inhibitors and some defensive specialized metabolites (caffeoylputrescine, diterpene glycosides) were lower in these plants [162]. Therefore, AtARGAH2 may affect caterpillar nutrition or plant defense.

The phloem-associated protein AtPP2-A5 has two domains, a PP2 (lectin activity) domain at the C-terminus and a Toll/Interleukin-1 receptor domain at the N-terminus [166]. Though this protein plays a major role in sealing wounded sieve elements (Pattern 1, Figure 5A), AtPP2-A5 overexpression or knockout lines show modified transcriptional patterns to spider mite herbivory, suggesting that the receptor portion of this protein recognizes an herbivore-specific effector to remodel gene expression [166]. The knockout line was more susceptible to spider mite damage, and the arthropods had higher mortality on the overexpression lines. This likely reflects direct interactions with the insect, potentially by binding to the arthropod gut epithelial [167]. Feeding aphids a diet spiked with recombinant AtPP2-A5 did not affect mortality but did negatively affect the weight gain of two different aphid species, the pea aphid *Acythosiphon pisum* (~30% smaller) and the green peach aphid *Myzus persicae* (10–20% smaller) [168]. Aphids reared on AtPP2-A5 overexpression lines had lower colonization and spent less time feeding on the phloem compared with WT plants [169].

Chlorophyllase, AtCHL1, catalyzes the hydrolysis of chlorophyll to chlorophyllide. Under stress conditions, this enzyme may be involved in chlorophyll degradation to minimize chlorophyll-associated ROS generation [170,171]. However, as this protein is associated with the endoplasmic reticulum or tonoplast, only upon cell disruption, such as that incurred by herbivory, does the enzyme come into contact with its substrate, chlorophyll. The product of this reaction, chlorophyllide, is toxic to *S. littoralis* caterpillars and

binds to the midgut of *Bombyx mori* caterpillars, potentially impairing digestion [172]. However, other studies suggest that chlorophyllide may have roles that benefit the insect herbivore [173]. In our study, *AtChl1* was induced late after wounding and showed higher expression in WT plants (Pattern 5, Figure 5E).

4. Materials and Methods

4.1. Plant Maintenance

Arabidopsis thaliana wildtype (WT) Columbia (Col-0) seeds were obtained from the Arabidopsis Biological Resource Center. Seeds of the *lox2-1* mutant line, which has a mutation in the tryptophan amino acid at position 630 to produce a stop codon resulting in a truncated non-functional protein, were generously provided by Dr. E. E. Farmer [28]. The seeds were surface-sterilized in 70% (*v/v*) ethanol for one min, then 0.6% (*v/v*) bleach (NaOCl) for 3 min, followed by five successive washes in sterile ddH₂O. Between these treatments, the seeds were recovered by centrifugation, and the liquid was removed. The seeds were then placed in Petri dishes containing Murashige and Skoog salts, pH 5.8, in 0.8% agar, followed by stratification in the dark at 4 °C to promote synchronized germination. After 2 days, the Petri dishes were transferred to a growth cabinet with 14 h of light with an intensity of 250 μmol m⁻² s⁻¹ followed by 10 h darkness. The temperature of the light–dark cycle was 23:20 °C. After one week, the germinated seedlings were transplanted into pots (12 cm diameter × 11 cm height) containing Fafard Agromix G6 potting medium and grown under the same conditions. Plants were bottom-watered 3 times per week with 20:20:20 NPK fertilizer (0.14 g/L distilled water) and used for experimentation at the vegetative 3.9 stage [174].

4.2. Experimental Design

Two days prior to the wounding experiment, a plexiglass sheet was placed between randomly chosen plants that were to remain unwounded or mechanically damaged to separate the treatments and avoid volatile signaling between these groups. At 9 PM (time 0; dark phase), arabidopsis lines were either mechanically damaged, whereby each leaf of the rosette was wounded once by a hole punch, without harming the mid-vein, or left unwounded. Whole rosettes were collected for phytohormones (1 h; dark phase), GSLs (12 h; light phase) or transcriptomics (1 h and 12 h, dark and light phase, respectively) post-damage, flash-frozen in liquid nitrogen and stored at –80 °C until analysis. The experiment was repeated temporally three times to collect samples for transcriptomics and five times for phytohormone and GSL analyses. At each temporal replicate, one sample was taken for the different analyses (RNA-Seq or metabolite analysis) of transcriptomics (n = 3), phytohormones (n = 5) and GSLs (n = 5).

4.3. Phytohormone Analysis

Following the protocol described in Martinez Henao et al. [175], plant samples were finely ground and extracted in ethyl acetate containing isotopically labeled standards (D6-JA, D6-JA-Ile and D4-SA (OChemim, s.r.o)). The samples were vigorously vortexed and centrifuged (19,000 × *g*, 10 min, 4 °C), and the supernatant was transferred to a new tube. The extraction was repeated, and the supernatants were pooled. Following evaporation using a vacuum concentrator at room temperature, the resulting pellet was resuspended in 70% (*v/v*) methanol (HPLC-MS grade). A final centrifugation step was performed as above to ensure the removal of all non-soluble debris. Metabolites were separated by ultrahigh performance liquid chromatography (UHPLC) followed by detection on a triple quadrupole mass spectrometer (EVOQ-TQ-MS, Bruker, Hamburg, Germany). Reverse phase UHPLC was performed using a Zorbax Extend-C18 column (4.6 × 50 mm, 1.8 μm, Agilent Technologies, Santa Clara, CA, USA). The mobile phase began with 5% (*v/v*) acetonitrile (ACN), 0.05% (*v/v*) formic acid for 30 s and then increased to 50% (*v/v*) ACN, 0.05% (*v/v*) formic acid over 2 min. After separation, the compounds were nebulized by electron spray ionization and detected using the EVOQ-TQ-MS. Phytohormones were

identified based on their retention time, in comparison with known standards, as well as their m/z .

4.4. Glucosinolate Analysis

GSLs were extracted from lyophilized leaf tissue and analyzed by high-performance liquid chromatography (HPLC)-pulsed amperometric detection following Grosser and van Dam [176]. Briefly, 70% MeOH was added to the finely ground tissues and incubated at 90 °C for 6 min to inactivate myrosinases followed by sonication for 15 min. After centrifugation ($2975 \times g$ for 10 min), the supernatant was transferred to a clean tube, and the pellet was re-extracted. Pooled supernatants were passed through a diethylaminoethyl Sephadex A-25 ion exchange column preconditioned with ddH₂O. After washing (2×1 mL 70% MeOH, 2×1 mL ddH₂O, 1×1 mL 20 mM sodium acetate buffer, pH 5.5), the column was treated with 10 U of arylsulfatase and incubated for 12 h at RT. Desulfated GSLs were eluted in sterile MilliQ H₂O (2×0.75 mL) and lyophilized.

GSLs were separated by reverse-phase chromatography on a C₁₈ column (Alltima C₁₈, 150×4.6 mm, 3 μ m, Alltech, Lexington, USA) using a mobile gradient from 2% acetonitrile (ACN) to 35% ACN in 30 min at a flow rate of 0.75 mL min⁻¹. GSLs were identified based on retention time to known standards (glucoiberin (3-methylsulfenylpropyl GSL), glucoerucin (4-methylthiobutyl GSL), progoinin (2-hydroxy-3-butenyl GSL), sinigrin (2-propenyl GSL), gluconapin (3-butenyl GSL), glucobrassicinapin (4-pentenyl GSL), glucobrassicin (indol-3-ylmethyl GSL), sinalbin (4-hydroxybenzyl GSL), glucotropaeolin (benzyl GSL) and gluconasturtiin (2-phenylethyl GSL); Phytoplan, Heidelberg, Germany) and UV spectra. GSL concentrations were calculated from a sinigrin standard curve according to Grosser and van Dam [176].

4.5. RNA Extraction, Library Preparation and Transcriptomics

Total RNA was extracted from flash-frozen pulverized plant rosettes (~100 mg) using the RNeasy Plant Mini Kit (Qiagen, Venlo, The Netherlands) following the manufacturer's protocol with an additional on-column DNase digestion step to avoid genomic DNA contamination. The 2100 Bioanalyzer instrument (Agilent Technologies) was used to determine RNA quality using an RNA integrity number (RIN) of 8.7 as a minimum threshold. Total RNA samples were processed by Genome Québec Innovation Centre for library preparation and next-generation RNA sequencing (RNA-Seq). Libraries were generated from 250 ng of total RNA as follows: mRNA enrichment and ribosomal RNA removal were performed using the Next Poly(A) Magnetic Isolation following the manufacturer's instructions (New England BioLabs, Ipswich, USA). cDNA synthesis was performed with Next RNA First Strand Synthesis and Next Ultra Directional RNA Second Strand Synthesis kits (New England BioLabs). The remaining steps of library preparation were performed using the Next Ultra II DNA Library Prep Kit for Illumina (New England BioLabs). Adapters and PCR primers were purchased from New England BioLabs.

The libraries were normalized, pooled and denatured in 0.02 N NaOH, followed by neutralization using HT1 hybridization buffer. Twenty-four strand-specific mRNA libraries were generated and sequenced by loading 200 pM on the NovaSeq 6000 S4 (Illumina) using the Xp protocol as per the manufacturer's recommendations, with paired-end (PE) mode for 2×100 base pairs (bp) resulting in >25 million reads in each direction. The Illumina phiX control v3 library was used as a control and mixed with libraries at a 1% level. Base calling was performed using Real-Time Analysis (RTA) v3 software. The program bcl2fastq v2.20 was used to demultiplex samples and generate fastq reads.

4.6. Quality Check, Clipping and Mapping

Raw read quality was examined by performing FastQC 0.11.9 on ".fastq.gz" file [177]. FastQC produces a control statistic and evaluates every metric using a classification system of pass, warn or fail. The adapter clipping and bad end quality trimming were performed by subjecting the raw reads to fastp tool version 0.20.1 to remove adapters,

low-quality bases with a Phred score less than 20 and reads shorter than 25 bp from the tail (3' end) from further analysis [178]. This preprocessing was followed by another quality check with FastQC. Read mapping was conducted using a splice-aware alignment tool STAR v2.7.9a to align the trimmed reads against the arabidopsis reference genome downloaded from The Arabidopsis Information Resource (TAIR, assembly ID: TAIR10, https://www.arabidopsis.org/download_files/Genes/TAIR10_genome_release/TAIR10_gff3/TAIR10_GFF3_genes.gff (accessed on 9 December 2022)) [179].

4.7. Differential Gene Expression

Strand-specific transcript abundance was calculated using featureCounts (a tool included in the subread package 2.0.3) on mapped and sorted BAM files. The resulting read counts per transcript values were imported into the web-based tool NetworkAnalyst 3.0 for data filtering, Log₂ normalization and differential analysis [180]. The statistical method DESeq2 with a negative binomial (Gamma–Poisson) distribution was used to identify differentially expressed genes using the log₂-fold change (logFC) calculation [181,182]. Genes with a False Discovery Rate (FDR)-corrected *p*-value (padj) ≤ 0.05 and log₂ fold change ≥ 2 or ≤ −2 were deemed significant. The transcriptomic data generated by this study are available in the Supplementary Materials of this article (Supplemental Table S1) and the raw read data (FASTQ) were deposited in the NCBI Sequence Read Archive (Bioproject ID #PRJNA1077722).

Transcriptomic visualization (ridgeplots, heatmaps, principal component analysis (PCA)) was performed using MetaboAnalyst 5.0 and ExpressAnalyst [183,184]. For visualization, the data were normalized by log₁₀ transformation.

4.8. Statistics

For phytohormone and GSL analyses, a two-factor analysis of variance (ANOVA) (factors: genotype and treatment) was conducted using the statistical program SPSS vers. 29 (Supplemental Tables S2 and S3).

5. Conclusions

By comparing early (1 h) and late (12 h) constitutive and wound responses between arabidopsis WT and *lox2* mutants, we identified gene expression differences related to the regulation of jasmonate biosynthesis and, in mechanically damaged plants, resistance to insect herbivores. Both constitutively and in wounded plants, SA levels are higher in *lox2*, which is reflected in the expression of SA-responsive genes. Since jasmonate and SA pathways are mutually antagonistic [106], this suggests that AtLOX2 may be involved in the constitutive biosynthesis of jasmonates that modulate SA levels.

As expected, the wound-associated jasmonate burst is dampened in *lox2* compared with WT plants. In the early response to wounding, genes are similarly expressed in both genotypes with few genotype-specific differences. In contrast, in the later transcriptional responses, higher expression of numerous genes involved in insect resistance is observed in WT plants compared to *lox2*, highlighting the role of AtLOX2 in arabidopsis resistance to insects (Figure 8).

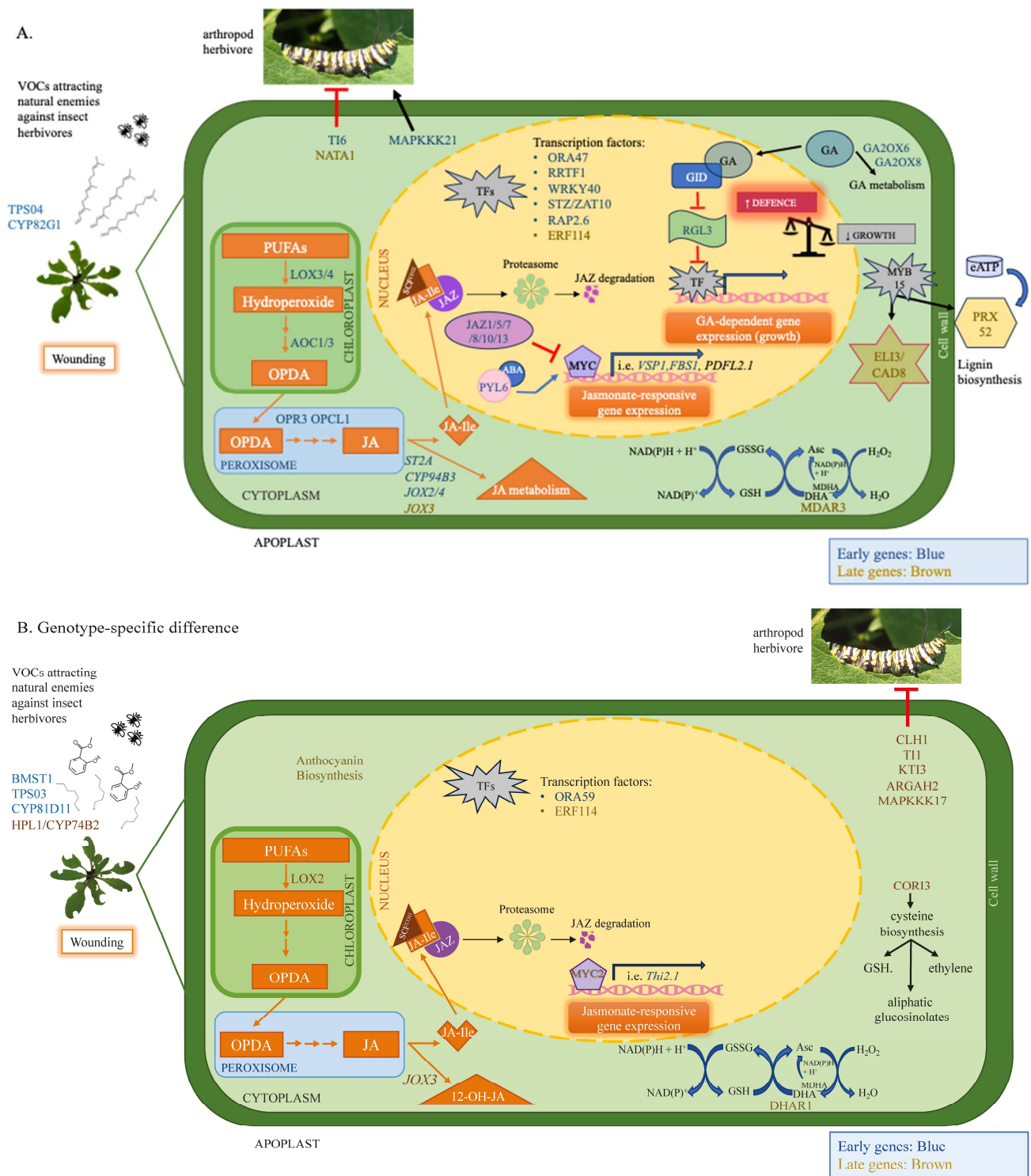


Figure 8. Wound-induced genes involved in plant–insect interactions in arabidopsis WT and *lox2* mutants. Foliar gene expression in wounded *lox2* mutants, which has a truncated non-functional enzyme, was compared to WT plants. Proteins encoded by early genes (1 h) are shown in blue, whereas later transcript expression (12 h) is depicted in brown. (A). General wound-induced responses found in both genotypes. Jasmonate biosynthesis begins in the chloroplast from 18C membrane lipid-derived precursors, typically α -linolenic acid, to finally form one of the biologically active jasmonates, jasmonoyl-isoleucine (JA-Ile). Numerous genes encoding enzymes in the jasmonate biosynthetic pathway are upregulated in wounded plants. JA-Ile enters the nucleus and forms a bridge between the SCF^{COI1} and jasmonate ZIM domain (JAZ) repressors, leading to their degradation through the

proteasome. The degradation of JAZ proteins releases MYC2/3/4 transcription factors, leading to jasmonate-responsive gene expression. The abscisic acid (ABA)-PYL6 receptor complex positively interacts with MYC2. Genes encoding JAZ-negative regulators as well as those further metabolizing jasmonic acid (JA) (i.e., JOX, ST2A) to inactive derivatives are also wound-induced. Gibberellin (GA) bound to its receptor GID1 activates a pathway that leads to the proteasome-mediated degradation of negative DELLA growth regulators, such as RGL3. In wounded leaves, the increase in *RGL3* expression and genes that encode GA2OX6 and GA2OX8, involved in gibberellin metabolism to inactive products, results in the suppression of plant growth. Numerous genes involved in oxidative stress are wound-induced. For example, the oxidative stress-associated transcription factor RRTF1 and MDAR3, which are part of the Foyer–Halliwell–Asada cycle, a series of interconnected enzymatic reactions to detoxify the reactive oxygen species hydrogen peroxide (H₂O₂). Wound-induced MYB15 leads to the expression of *ELI3/CAD8* and *PRX52*, which contribute to lignin biosynthesis. TPS04 and CYP82G1 are involved in the biosynthesis of volatiles, such as 4,8,12-trimethyltrideca-1,3,7,11-tetraene (TMTT), that are attractive to natural enemies of the herbivorous insect. TI1 and NATA1 contribute to plant resistance against arthropods, whereas MAPKKK21 is a negative regulator of arthropod resistance. (B). LOX2-specific responses. Wound-induced genes expressed at higher levels in WT compared with *lox2* plants. Wound-induced expression of genes that encode LOX2 and MYC2 involved in jasmonate biosynthesis and signaling, respectively, is noted. COR13 is a cysteine lyase involved in cysteine biosynthesis that produces precursors for ethylene, aliphatic glucosinolates (GSLs) and reduced glutathione (GSH) involved in the Foyer–Halliwell–Asada cycle. Also, the expression of the gene encoding DHAR1 in this pathway is wound-induced. Other cellular antioxidants whose biosynthetic pathway is positively regulated in these plants are anthocyanins. Indirect defenses involved in volatile biosynthesis are wound-induced. An increase the genes that encode proteins involved in antinutritive defenses, such as CLH1, ARGAH2 and TIs, as well as MAPKKK17, an important signaling kinase involved in arthropod resistance, is also seen. Abbreviations: ABA: abscisic acid, AOC: allene oxide cyclase, AOS: allene oxide synthase, DHAR1: dehydroascorbate reductase1, GA: gibberellin, GSH: reduced glutathione, GSL: glucosinolate, GSSG: oxidized glutathione, JA: jasmonic acid, JA-Ile: jasmonoyl-isoleucine, JAZ: jasmonate-Zim domain, JOX: jasmonate oxidase, LOX: lipoxygenase, OPDA: 12-*oxo*-phytodienoic acid, OPR: *oxo*-phytodienoate reductase, OPCL: OPC-8-CoA ligase, PUFA: polyunsaturated fatty acid, TF: transcription factor, TMTT: 4,8,12-trimethyltrideca-1,3,7,11-tetraene.

Supplementary Materials: The following supporting information can be downloaded at: <https://www.mdpi.com/article/10.3390/ijms25115898/s1>.

Author Contributions: The experimental design was conceived by D.K. and J.C.B. and conducted by D.K. (wounding experiments, transcriptomic analyses), J.M.H. (transcriptomic analyses) and C.L. (molecular training) under the supervision of J.R. and J.C.B. The phytohormone analysis was conducted by A.S. under the supervision of N.M.v.D. The data were analyzed and this manuscript was written by D.K. and J.C.B., with valuable input from J.M.H., C.L., A.S., N.M.v.D. and J.R. All authors have read and agreed to the published version of the manuscript.

Funding: We gratefully acknowledge our funding sources for supporting this research including the Deutsche Forschungsgemeinschaft (DFG-FZT 118, 202548816) (NMvD, AS), the Natural Science and Engineering Research Council (NSERC) Discovery grants (NSERC-2019-04516 to JCB and NSERC-2019-05955 to JR), and the Fonds de recherche du Québec—nature et technologies (FRQNT) Centre SÈVE (FRQNT-RQT00335) to JCB and JR.

Institutional Review Board Statement: Not applicable.

Informed Consent Statement: Not applicable.

Data Availability Statement: The data that support the findings of this study are available within this article. The transcriptomic data (FASTQ) generated by this study are available through the NCBI Sequence Read Archive (Bioproject ID #PRJNA1077722).

Acknowledgments: We are grateful to Edward Farmer for providing the background *lox2-1* mutant lines. We thank Genome Québec for the preparation of the RNA libraries and RNA-Seq analyses as well as Compute Canada and the Digital Alliance of Canada (alliancecan.ca) for computational support.

Conflicts of Interest: The authors declare that this research was conducted in the absence of any commercial or financial relationships that could be construed as a potential conflict of interest.

Abbreviations

ABA: abscisic acid, ACN: acetonitrile, ANOVA: analysis of variance, AOC: allene oxide cyclase, AOS: allene oxide synthase, BPs: base pairs, Col-0: Columbia, DEGs: differentially expressed genes, EDS1: enhanced disease susceptibility 1, GSH: reduced glutathione, GSSG: oxidized glutathione, JA-Ile: (+)-7-*iso*-jasmonoyl-isoleucine, JAR1: jasmonate resistant1, JAZ: jasmonate zim domain, KOBAS: KEGG orthology-based annotation system, LOX: lipoxygenase, MACP: membrane attack complex/perforin, OPDA: (9S,13S)-12-*oxo*-phytodienoic acid, PCA: principal component analysis, PE: paired-end, PR1: pathogenesis-related 1, RIN: RNA integrity number, RNA-Seq: RNA sequencing, ROS: reactive oxygen species, TIR-NBS-LRR: toll interleukin receptor–nucleotide binding site–leucine-rich repeat, UHPLC-EVOQ-TQ-MS: ultrahigh performance liquid chromatography–Evoq–triple quadrupole–mass spectrometry, VOCs: volatile organic compounds, VSP: vegetative storage protein.

References

1. Wasternack, C.; Hause, B. Jasmonates: Biosynthesis, perception, signal transduction and action in plant stress response, growth and development. An update to the 2007 review in *Annals of Botany*. *Ann. Bot.* **2013**, *111*, 1021–1058. [[CrossRef](#)] [[PubMed](#)]
2. Jang, G.; Yoon, Y.; Do Choi, Y. Crosstalk with jasmonic acid integrates multiple responses in plant development. *Int. J. Mol. Sci.* **2020**, *21*, 305. [[CrossRef](#)] [[PubMed](#)]
3. Zhang, L.; Zhang, F.; Melotto, M.; Yao, J.; He, S.Y. Jasmonate signaling and manipulation by pathogens and insects. *J. Exp. Bot.* **2017**, *68*, 1371–1385. [[CrossRef](#)] [[PubMed](#)]
4. Wasternack, C.; Song, S. Jasmonates: Biosynthesis, metabolism, and signaling by proteins activating and repressing transcription. *J. Exp. Bot.* **2017**, *68*, 1308–1321. [[CrossRef](#)] [[PubMed](#)]
5. Li, H.-M.; Yu, C.-W. Chloroplast galactolipids: The link between photosynthesis, chloroplast shape, jasmonates, phosphate starvation and freezing tolerance. *Plant Cell Physiol.* **2018**, *59*, 1128–1134. [[CrossRef](#)] [[PubMed](#)]
6. Stenzel, I.; Hause, B.; Miersch, O.; Kurz, T.; Maucher, H.; Weichert, H.; Ziegler, J.; Feussner, I.; Wasternack, C. Jasmonate biosynthesis and the allene oxide cyclase family of *Arabidopsis thaliana*. *Plant Mol. Biol.* **2003**, *51*, 895–911. [[CrossRef](#)]
7. Farmer, E.E.; Goossens, A. Jasmonates: What ALLENE OXIDE SYNTHASE does for plants. *J. Exp. Bot.* **2019**, *70*, 3373–3378. [[CrossRef](#)] [[PubMed](#)]
8. Guan, L.; Denkert, N.; Eisa, A.; Lehmann, M.; Sjuts, I.; Weiberg, A.; Soll, J.; Meinecke, M.; Schwenkert, S. Jassy, a chloroplast outer membrane protein required for jasmonate biosynthesis. *Proc. Natl. Acad. Sci. USA* **2019**, *116*, 10568–10575. [[CrossRef](#)] [[PubMed](#)]
9. Theodoulou, F.L.; Job, K.; Slocombe, S.P.; Footitt, S.; Holdsworth, M.; Baker, A.; Larson, T.R.; Graham, I.A. Jasmonic acid levels are reduced in COMATOSE ATP-binding cassette transporter mutants. Implications for transport of jasmonate precursors into peroxisomes. *Plant Physiol.* **2005**, *137*, 835–840. [[CrossRef](#)]
10. Wang, F.; Yu, G.; Liu, P. Transporter-mediated subcellular distribution of the metabolism and signaling of jasmonates. *Front. Plant Sci.* **2019**, *10*, 390. [[CrossRef](#)]
11. Staswick, P.E.; Tiryaki, I. The oxylipin signal jasmonic acid is activated by an enzyme that conjugates it to isoleucine in *Arabidopsis*. *Plant Cell* **2004**, *16*, 2117–2127. [[CrossRef](#)] [[PubMed](#)]
12. Fonseca, S.; Chini, A.; Hamberg, M.; Adie, B.; Porzel, A.; Kramell, R.; Miersch, O.; Wasternack, C.; Solano, R. (+)-7-*iso*-jasmonoyl-L-isoleucine is the endogenous bioactive jasmonate. *Nat. Chem. Biol.* **2009**, *5*, 344–350. [[CrossRef](#)]
13. Thines, B.; Katsir, L.; Melotto, M.; Niu, Y.; Mandaokar, A.; Liu, G.; Nomura, K.; He, S.Y.; Howe, G.A.; Browse, J. JAZ repressor proteins are targets of the SCF^{COI1} complex during jasmonate signalling. *Nature* **2007**, *448*, 661–665. [[CrossRef](#)] [[PubMed](#)]
14. Sheard, L.B.; Tan, X.; Mao, H.; Withers, J.; Ben-Nissan, G.; Hinds, T.R.; Kobayashi, Y.; Hsu, F.F.; Sharon, M.; He, S.Y.; et al. Jasmonate perception by inositol-phosphate-potentiated COI1-JAZ co-receptor. *Nature* **2010**, *468*, 400–405. [[CrossRef](#)] [[PubMed](#)]
15. Li, Q.; Zheng, J.; Li, S.; Huang, G.; Skilling, S.J.; Wang, L.; Li, L.; Li, M.; Yuan, L.; Liu, P. Transporter-mediated nuclear entry of jasmonoyl-isoleucine is essential for jasmonate signaling. *Mol. Plant* **2017**, *10*, 695–708. [[CrossRef](#)] [[PubMed](#)]
16. Zhai, Q.; Deng, L.; Li, C. Mediator subunit MED25: At the nexus of jasmonate signaling. *Curr. Opin. Plant Biol.* **2020**, *57*, 78–86. [[CrossRef](#)] [[PubMed](#)]
17. Takaoka, Y.; Suzuki, K.; Nozawa, A.; Takahashi, H.; Sawasaki, T.; Ueda, M. Protein–protein interactions between jasmonate-related master regulator MYC and transcriptional mediator MED25 depend on a short binding domain. *J. Biol. Chem.* **2022**, *298*, 101504. [[CrossRef](#)] [[PubMed](#)]
18. Hopkins, R.J.; van Dam, N.M.; van Loop, J.J.A. Role of glucosinolates in insect-plant relationships and multitrophic interactions. *Annu. Rev. Entomol.* **2009**, *54*, 57–83. [[CrossRef](#)] [[PubMed](#)]
19. Mitreiter, S.; Gigolashvili, T. Regulation of glucosinolate biosynthesis. *J. Exp. Bot.* **2021**, *72*, 70–91. [[CrossRef](#)]

20. Liu, B.; Seong, K.; Pang, S.; Song, J.; Gao, H.; Wang, C.; Zhai, J.; Zhang, Y.; Gao, S.; Li, X.; et al. Functional specificity, diversity, and redundancy of *Arabidopsis* JAZ family repressors in jasmonate and COI1-regulated growth, development, and defense. *New Phytol.* **2021**, *231*, 1525–1545. [[CrossRef](#)]
21. Burow, M.; Hilkie, B.A. How does a plant orchestrate defense in time and space? Using glucosinolates in *Arabidopsis* as a case study. *Curr. Opin. Plant Biol.* **2017**, *38*, 142–147. [[CrossRef](#)] [[PubMed](#)]
22. Beekwilder, J.; van Leeuwen, W.; van Dam, N.M.; Bertossi, M.; Grandi, V.; Mizzi, L.; Soloviev, M.; Szabados, L.; Molthoff, J.W.; Schipper, B.; et al. The impact of the absence of aliphatic glucosinolates on insect herbivory in *Arabidopsis*. *PLoS ONE* **2008**, *3*, e2068. [[CrossRef](#)] [[PubMed](#)]
23. Kim, J.H.; Lee, B.W.; Schroeder, F.C.; Jander, G. Identification of indole glucosinolate breakdown products with antifeedent effects on *Myzus persicae* (green peach aphid). *Plant J.* **2008**, *54*, 1015–1026. [[CrossRef](#)] [[PubMed](#)]
24. Müller, R.; de Vos, M.; Sun, J.Y.; Sønderby, I.E.; Halkier, B.A.; Wittstock, U.; Jander, G. Differential effects of indole and aliphatic glucosinolates on lepidopteran herbivores. *J. Chem. Ecol.* **2010**, *36*, 905–913. [[CrossRef](#)]
25. Jeschke, V.; Kearney, E.E.; Schramm, K.; Kunert, G.; Shekhov, A.; Gershenzon, J.; Vassão, D.G. How glucosinolates affect generalist lepidopteran larvae: Growth, development and glucosinolate metabolism. *Front. Plant Sci.* **2017**, *8*, 1995. [[CrossRef](#)] [[PubMed](#)]
26. Jeschke, V.; Zalucki, J.M.; Raguschke, B.; Gershenzon, J.; Heckel, D.G.; Zalucki, M.P.; Vassão, D.G. So much for glucosinolates: A generalist does survive and develop on Brassicas, but at what cost. *Plants* **2021**, *10*, 962. [[CrossRef](#)] [[PubMed](#)]
27. Glauser, G.; Grata, E.; Dubugnon, L.; Rudaz, S.; Farmer, E.E.; Wolfender, J.L. Spatial and temporal dynamics of jasmonate synthesis and accumulation in *Arabidopsis* in response to wounding. *J. Biol. Chem.* **2008**, *283*, 16400–16407. [[CrossRef](#)] [[PubMed](#)]
28. Glauser, G.; Dubugnon, L.; Mousavi, S.A.; Rudaz, S.; Wolfender, J.L.; Farmer, E.E. Velocity estimates for signal propagation leading to systemic jasmonic acid accumulation in wounded *Arabidopsis*. *J. Biol. Chem.* **2009**, *284*, 34506–34513. [[CrossRef](#)] [[PubMed](#)]
29. Scholz, S.S.; Reichelt, M.; Boland, W.; Mithöfer, A. Additional evidence against jasmonate-induced jasmonate induction hypothesis. *Plant Sci.* **2015**, *239*, 9–14. [[CrossRef](#)]
30. Schaller, A.; Stintzi, A. Jasmonate biosynthesis and signaling for induced plant defense against herbivory. In *Induced Plant Resistance to Herbivores*; Schaller, A., Ed.; Springer: Dordrecht, The Netherlands, 2008; pp. 349–366. [[CrossRef](#)]
31. Thivierge, K.; Prado, A.; Driscoll, B.T.; Bonneil, É.; Thibault, P.; Bede, J.C. Caterpillar- and salivary-specific modification of plant proteins. *J. Proteome Res.* **2010**, *9*, 5887–5895. [[CrossRef](#)]
32. Kaur, D.; Dorion, S.; Jmii, S.; Cappadocia, L.; Bede, J.C.; Rivoal, J. Pseudophosphorylation of *Arabidopsis* jasmonate biosynthesis enzyme lipoxygenase 2 via mutation of Ser⁶⁰⁰ inhibits enzyme activity. *J. Biol. Chem.* **2023**, *299*, 102898. [[CrossRef](#)]
33. Chauvin, A.; Lenglet, A.; Wolfender, J.L.; Farmer, E.E. Paired hierarchical organization of 13-lipoxygenases in *Arabidopsis*. *Plants* **2016**, *5*, 16. [[CrossRef](#)]
34. Prasad, A.; Sedlářová, M.; Kale, R.S.; Pospíšil, P. Lipoxygenase in singlet oxygen generation as a response to wounding: In vivo imaging in *Arabidopsis thaliana*. *Sci. Rep.* **2017**, *7*, 9831. [[CrossRef](#)] [[PubMed](#)]
35. Prasad, A.; Sedlářová, M.; Balukova, A.; Rác, M.; Pospíšil, P. Reactive oxygen species as a response to wounding: In vivo imaging in *Arabidopsis thaliana*. *Front. Plant Sci.* **2020**, *10*, 1660. [[CrossRef](#)]
36. Bannenberg, G.; Martínez, M.; Hamberg, M.; Castresana, C. Diversity of the enzymatic activity in the lipoxygenase gene family of *Arabidopsis thaliana*. *Lipids* **2009**, *44*, 85–95. [[CrossRef](#)] [[PubMed](#)]
37. Lefevre, H.; Bauters, L.; Gheysen, G. Salicylic acid biosynthesis in plants. *Front. Plant Sci.* **2020**, *11*, 338. [[CrossRef](#)]
38. Blanco, F.; Salinas, P.; Cecchini, N.M.; Jordana, X.; Van Hummelen, P.; Alvarez, M.E.; Holuigue, L. Early genomic responses to salicylic acid in *Arabidopsis*. *Plant Mol. Biol.* **2009**, *70*, 79–102. [[CrossRef](#)] [[PubMed](#)]
39. Schaller, A.; Stintzi, A. Enzymes in jasmonate biosynthesis—Structure, function, regulation. *Phytochemistry* **2009**, *70*, 1532–1538. [[CrossRef](#)] [[PubMed](#)]
40. Fernández-Calvo, P.; Chini, A.; Fernández-Barbero, G.; Chico, J.M.; Gimenez-Ibanez, S.; Geerinck, J.; Eckhout, D.; Schweizer, F.; Godoy, M.; Franco-Zorrilla, J.M.; et al. The *Arabidopsis* bHLH transcription factors MYC3 and MYC4 are targets of JAZ repressors and act additively with MYC2 in the activation of jasmonate responses. *Plant Cell* **2011**, *23*, 701–715. [[CrossRef](#)]
41. Zeng, L.; Chen, H.; Wang, Y.; Hicks, D.; Ke, H.; Pruneda-Paz, J.; Dehesh, K. ORA47 is a transcriptional regulator of a general stress response hub. *Plant J.* **2022**, *110*, 562–571. [[CrossRef](#)]
42. Pauwels, L.; Goossens, A. The JAZ proteins: A crucial interface in the jasmonate signaling cascade. *Plant Cell* **2011**, *23*, 3089–3100. [[CrossRef](#)] [[PubMed](#)]
43. Liu, Z.; Wang, H.; Xie, J.; Lv, J.; Zhang, G.; Hu, L.; Luo, S.; Li, L.; Yu, J. The roles of cruciferae glucosinolates in disease and pest resistance. *Plants* **2021**, *10*, 1097. [[CrossRef](#)] [[PubMed](#)]
44. Heitz, T.; Widemann, E.; Lugan, R.; Miesch, L.; Ullmann, P.; Désaubry, L.; Holder, E.; Grausem, B.; Kandel, S.; Miesch, M.; et al. Cytochromes P450 CYP94C1 and CYP94B3 catalyze two successive oxidation steps of plant hormone jasmonoyl-isoleucine for catabolic turnover. *J. Biol. Chem.* **2012**, *287*, 6296–6306. [[CrossRef](#)] [[PubMed](#)]
45. Widemann, E.; Miesch, L.; Lugan, R.; Holder, E.; Heinrich, C.; Aubert, Y.; Miesch, M.; Pinot, F.; Heitz, T. The amidohydrolases IAR3 and ILL6 contribute to jasmonoyl-isoleucine hormone turnover and generate 12-hydroxyjasmonic acid upon wounding in *Arabidopsis* leaves. *J. Biol. Chem.* **2013**, *288*, 31701–31714. [[CrossRef](#)] [[PubMed](#)]

46. Caarls, L.; Elberse, J.; Awwanah, M.; Ludwig, N.R.; De Vries, M.; Zeilmaker, T.; Van Wees, S.C.; Schuurink, R.C.; Van den Ackerveken, G. *Arabidopsis* JASMONATE-INDUCED OXYGENASES down-regulate plant immunity by hydroxylation and inactivation of the hormone jasmonic acid. *Proc. Natl. Acad. Sci. USA* **2017**, *114*, 6388–6393. [[CrossRef](#)] [[PubMed](#)]
47. Smirnova, E.; Marquis, V.; Poirier, L.; Aubert, Y.; Zumsteg, J.; Ménard, R.; Miesch, L.; Heitz, T. Jasmonic acid oxidase 2 hydroxylates jasmonic acid and represses basal defense and resistance responses against *Botrytis cinerea* infection. *Mol. Plant* **2017**, *10*, 1159–1173. [[CrossRef](#)] [[PubMed](#)]
48. Yi, R.; Du, R.; Wang, J.; Yan, J.; Chu, J.; Yan, J.; Shan, X.; Xie, D. Dioxygenase JID1 mediates the modification of OPDA to regulate jasmonate homeostasis. *Cell Discov.* **2023**, *9*, 29. [[CrossRef](#)] [[PubMed](#)]
49. Lee, S.; Badieyan, S.; Bevan, D.R.; Herde, M.; Gatz, C.; Tholl, D. Herbivore-induced and floral homoterpene volatiles are biosynthesized by a single P450 enzyme (CYP82G1) in *Arabidopsis*. *Proc. Natl. Acad. Sci. USA* **2010**, *107*, 21205–21210. [[CrossRef](#)] [[PubMed](#)]
50. Parker, M.T.; Zhong, Y.; Dai, X.; Wang, S.; Zhao, P. Comparative genomic and transcriptomic analysis of terpene synthases in *Arabidopsis* and *Medicago*. *IET Syst. Biol.* **2013**, *8*, 146–153. [[CrossRef](#)]
51. Woolfson, K.N.; Esfandiari, M.; Bernards, M.A. Suberin biosynthesis, assembly, and regulation. *Plants* **2022**, *11*, 555. [[CrossRef](#)]
52. Krishnamurthy, S.; Verma, S.; Rahman, M.H.; Kav, N.N.V. Functional characterization of four APETALA2-family genes (*RAP2.6*, *RAP2.6L*, *DREB19* and *DREB26*) in *Arabidopsis*. *Plant Mol. Biol.* **2011**, *75*, 107–127. [[CrossRef](#)] [[PubMed](#)]
53. Matsuo, M.; Johnson, J.M.; Hieno, A.; Tokizawa, M.; Nomoto, M.; Tada, Y.; Godfrey, R.; Obokata, J.; Sherameti, I.; Yamamoto, Y.Y.; et al. High REDOX RESPONSIVE TRANSCRIPTION FACTOR1 levels result in accumulation of reactive oxygen species in *Arabidopsis thaliana* shoots and roots. *Mol. Plant* **2015**, *8*, 1253–1273. [[CrossRef](#)] [[PubMed](#)]
54. Matsuo, M.; Oelmüller, R. REDOX RESPONSIVE TRANSCRIPTION FACTOR1 is involved in age-dependent and systemic stress signaling. *Plant Signal. Behav.* **2015**, *10*, e1051279. [[CrossRef](#)] [[PubMed](#)]
55. Dong, X.; Zhu, R.; Kang, E.; Shang, Z. RRFT1 (Redox Responsive Transcription Factor 1) is involved in extracellular ATP-regulated gene expression in *Arabidopsis thaliana* seedlings. *Plant Signal. Behav.* **2020**, *15*, 1748282. [[CrossRef](#)] [[PubMed](#)]
56. Pandey, S.P.; Roccaro, M.; Schön, M.; Logemann, E.; Somssich, I.E. Transcriptional reprogramming regulated by WRKY18 and WRKY40 facilitates powdery mildew infection of *Arabidopsis*. *Plant J.* **2020**, *64*, 912–923. [[CrossRef](#)] [[PubMed](#)]
57. Jongsema, M.A.; Beekwilder, J. Plant Protease Inhibitors: Functional Evolution for Defense. In *Induced Plant Resistance to Herbivores*; Schaller, A., Ed.; Springer: Dordrecht, The Netherlands, 2008; pp. 235–251. [[CrossRef](#)]
58. Romero-Hernandez, G.; Martinez, M. Opposite roles of MAPKKK17 and MAPKKK21 against *Tetranychus urticae* in *Arabidopsis*. *Front. Plant Sci.* **2022**, *13*, 5057. [[CrossRef](#)] [[PubMed](#)]
59. Rieu, I.; Ruiz-Rivero, O.; Fernandez-Garcia, N.; Griffiths, J.; Powers, S.J.; Gong, F.; Linhartova, T.; Eriksson, S.; Nilsson, O.; Thomas, S.G.; et al. The gibberellin biosynthetic genes *AtGA20ox1* and *AtGA20ox2* act, partially redundantly, to promote growth and development throughout the *Arabidopsis* life cycle. *Plant Cell* **2008**, *53*, 488–504. [[CrossRef](#)]
60. Wild, M.; Davière, J.-M.; Cheminant, S.; Regnault, T.; Baumbergerm, N.; Heintz, D.; Baltz, R.; Genschik, P.; Achard, P. The *Arabidopsis* *DELLA RGA-LIKE3* is a direct target of MYC2 and modulates jasmonate signaling responses. *Plant Cell* **2012**, *24*, 3307–3319. [[CrossRef](#)] [[PubMed](#)]
61. Thomas, S.G.; Blázquez, M.A.; Alabadi, D. *DELLA* proteins: Master regulators of gibberellin-responsive growth and development. *Annu. Plant Rev.* **2016**, *49*, 189–228. [[CrossRef](#)]
62. Wasternack, C. A plant's balance of growth and defense—Revisited. *New Phytol.* **2017**, *215*, 1291–1294. [[CrossRef](#)]
63. Kiyosue, T.; Yamaguchi-Shinozaki, Y.; Shinozaki, K. Characterization of two cDNAs (*ERD₁₀* and *ERD₁₄*) corresponding to genes that respond rapidly to dehydration stress in *Arabidopsis thaliana*. *Plant Cell Physiol.* **1994**, *35*, 225–231. [[CrossRef](#)]
64. Ren, Z.; Zheng, Z.; Chinnusamy, V.; Zhu, J.; Cui, X.; Iida, K.; Zhu, J.-K. *RAS1*, a quantitative trait locus for salt tolerance and ABA sensitivity in *Arabidopsis*. *Proc. Natl. Acad. Sci. USA* **2010**, *107*, 5669–5674. [[CrossRef](#)]
65. Aleman, F.; Yazaki, J.; Lee, M.; Takahashi, Y.; Kim, A.Y.; Li, Z.; Kinoshita, T.; Ecker, J.R.; Schroeder, J.I. An ABA-increased interaction of the *PYL6* ABA receptor with MYC2 transcription factor: A putative link of ABA and JA signaling. *Sci. Rep.* **2016**, *6*, 28941. [[CrossRef](#)] [[PubMed](#)]
66. de Dios Barajas-Lopez, J.; Tiwari, A.; Zarza, X.; Shaw, M.W.; Pascual, J.; Punkkinen, M.; Bakowska, J.C.; Munnik, T.; Fujii, H. EARLY RESPONSE TO DEHYDRATION 7 remodels cell membrane lipid composition during cold stress in *Arabidopsis*. *Plant Cell Physiol.* **2021**, *62*, 80–91. [[CrossRef](#)] [[PubMed](#)]
67. Zhang, X.; Cheng, X.; Zhang, C.; Ma, X.; Zhang, Y.; Song, J.; Xie, M. Genome-wide analysis of hyperosmolality-gated calcium-permeable channel (OSCA) family members and their involvement in various osmotic stresses in *Brassica napus*. *Gene* **2023**, *856*, 147137. [[CrossRef](#)]
68. Ton, J.; Flors, V.; Mauch-Mani, B. The multifaceted role of ABA in disease resistance. *Trends Plant Sci.* **2009**, *14*, 310–317. [[CrossRef](#)]
69. Nguyen, D.; Rieu, I.; Mariani, C.; van Dam, N.M. How plants handle multiple stresses: Hormonal interactions underlying responses to abiotic stress and insect herbivory. *Plant Mol. Biol.* **2016**, *91*, 27–740. [[CrossRef](#)] [[PubMed](#)]
70. Chapman, K.M.; Marchi-Werle, L.; Hunt, T.E.; Heng-Moss, T.M.; Louis, J. Abscisic and jasmonic acids contribute to soybean tolerance to the soybean aphid (*Aphis glycines* Matsumura). *Sci. Rep.* **2018**, *8*, 15148. [[CrossRef](#)]
71. Zhu, Z. Molecular basis for jasmonate and ethylene signal interactions in *Arabidopsis*. *J. Exp. Bot.* **2014**, *65*, 5743–5748. [[CrossRef](#)]
72. Meskauskiene, R.; Nater, M.; Goslings, D.; Kessler, F.; op den Camp, R.; Apel, K. Flu: A negative regulator of chlorophyll biosynthesis in *Arabidopsis thaliana*. *Proc. Natl. Acad. Sci. USA* **2001**, *98*, 12826–12831. [[CrossRef](#)]

73. op den Camp, R.G.; Przybyla, D.; Ochsenbein, C.; Laloi, C.; Kim, C.; Danon, A.; Wagner, D.; Hideg, É.; Göbel, C.; Feussner, I.; et al. Rapid induction of distinct stress responses after the release of singlet oxygen in arabidopsis. *Plant Cell* **2003**, *15*, 2320–2332. [[CrossRef](#)] [[PubMed](#)]
74. Memelink, J. Regulation of gene expression by jasmonate hormones. *Phytochemistry* **2009**, *70*, 156–1570. [[CrossRef](#)]
75. Bohlmann, H.; Vignutelli, A.; Hilpert, B.; Miersch, O.; Wasternack, C.; Apel, K. Wounding and chemicals induce expression of the *Arabidopsis thaliana* gene Thi2.1, encoding a fungal defense thionin, via the octadecanoid pathway. *FEBS Lett.* **1998**, *437*, 281–286. [[CrossRef](#)]
76. Huang, M.; Abel, C.; Sohrabi, R.; Petri, J.; Haupt, I.; Cosimano, J.; Gershenzon, J.; Tholl, D. Variation of herbivore-induced volatile terpenes among arabidopsis ecotypes depends on allelic differences and subcellular targeting of two terpene synthases, TPS02 and TPS03. *Plant Physiol.* **2010**, *153*, 1293–1310. [[CrossRef](#)]
77. Matthes, M.; Bruce, T.; Chamberlain, K.; Pickett, J.; Napier, J. Emerging roles in plant defense for cis-jasmone-induced cytochrome P450 CYP81D11. *Plant Signal. Behav.* **2011**, *6*, 563–565. [[CrossRef](#)]
78. Köster, J.; Thurrow, C.; Kruse, K.; Meier, A.; Ivan, T.; Feussner, I.; Gatz, C. Xenobiotic- and jasmonic acid-inducible signal transduction pathway have become interdependent at the *Arabidopsis CYP81D11* promoter. *Plant Physiol.* **2012**, *159*, 391–402. [[CrossRef](#)] [[PubMed](#)]
79. Rate, D.N.; Cuenca, J.V.; Bowman, G.R.; Guttman, D.S.; Greenberg, J.T. The gain-of-function arabidopsis *acd6* mutant reveals novel regulation and function of salicylic acid signaling pathway in controlling cell death, defenses, and cell growth. *Plant Cell* **1999**, *11*, 1695–1708. [[CrossRef](#)] [[PubMed](#)]
80. Acharya, B.R.; Raina, S.; Maqbool, S.B.; Jagadeeswaran, G.; Mosher, S.L.; Appel, H.M.; Schultz, J.C.; Klessig, D.F.; Raina, R. Overexpression of CRK13, an Arabidopsis cysteine-rich receptor-like kinase, results in enhanced resistance to *Pseudomonas syringae*. *Plant J.* **2007**, *50*, 488–499. [[CrossRef](#)]
81. Raes, J.; Rohde, A.; Christensen, J.H.; Van de Peer, Y.; Boerjan, W. Genome-wide characterization of the lignification toolbox in Arabidopsis. *Plant Physiol.* **2003**, *133*, 1051–1071. [[CrossRef](#)]
82. Hoffmann, N.; Benske, A.; Betz, H.; Schuetz, M.; Samuels, A.L. Laccases and peroxidases co-localize in lignified secondary cell walls throughout stem development. *Plant Physiol.* **2020**, *184*, 806–822. [[CrossRef](#)]
83. Ameye, M.; Allmann, S.; Verwaeren, J.; Smaghe, G.; Haesaert, G.; Schuurink, R.C.; Audenaert, K. Green leaf volatile production by plants: A meta-analysis. *New Phytol.* **2018**, *220*, 666–683. [[CrossRef](#)]
84. Tsuchiya, T.; Ohta, H.; Okawa, K.; Iwamatsu, A.; Shimada, H.; Masuda, T.; Takamiya, K.-I. Cloning of chlorophyllase, the key enzyme in chlorophyll degradation: Finding of a lipase motif and the induction by methyl jasmonate. *Proc. Natl. Acad. Sci. USA* **1999**, *96*, 15362–15367. [[CrossRef](#)]
85. Brownfield, D.L.; Todd, C.D.; Deyholos, M.K. Analysis of *Arabidopsis* arginase gene transcription patterns indicates specific biological functions for recently diverged paralogs. *Plant Mol. Biol.* **2008**, *67*, 429–440. [[CrossRef](#)] [[PubMed](#)]
86. Chen, H.; Wilkerson, C.G.; Kuchar, J.A.; Phinney, B.S.; Howe, G.A. Jasmonate-inducible plant enzymes degrade essential amino acids in the herbivore midgut. *Proc. Natl. Acad. Sci. USA* **2005**, *102*, 19237–19242. [[CrossRef](#)] [[PubMed](#)]
87. Ding, H.; Wang, B.; Han, Y.; Li, S. The pivotal function of dehydroascorbate reductase in glutathione homeostasis in plants. *J. Exp. Bot.* **2020**, *71*, 3405–3416. [[CrossRef](#)]
88. Gonzalez, A.; Zhao, M.; Leavitt, J.M.; Lloyd, A.M. Regulation of the anthocyanin biosynthetic pathway by the TTG1/bHLH/Myb transcription complex in Arabidopsis seedlings. *Plant J.* **2008**, *53*, 814–827. [[CrossRef](#)]
89. Shan, X.; Zhang, Y.; Peng, W.; Wang, Z.; Xie, D. Molecular mechanism for jasmonate-induction of anthocyanin accumulation in Arabidopsis. *J. Exp. Bot.* **2009**, *60*, 3849. [[CrossRef](#)] [[PubMed](#)]
90. Cappellini, F.; Marinelli, A.; Toccaceli, M.; Tonelli, C.; Petroni, K. Anthocyanins: From mechanisms of regulation in plants to health benefits in foods. *Front. Plant Sci.* **2021**, *12*, 748049. [[CrossRef](#)] [[PubMed](#)]
91. Payne, T.C.; Zhang, F.; Lloyd, A.M. *GL3* encodes a bHLH protein that regulates trichome development in arabidopsis through interaction with GL1 and TTG1. *Genetics* **2000**, *156*, 1349–1362. [[CrossRef](#)]
92. Jakab, G.; Manrique, A.; Zimmerli, L.; Métraux, J.-P.; Mauch-Mani, B. Molecular characterization of a novel lipase-like pathogen-inducible gene family of Arabidopsis. *Plant Physiol.* **2003**, *132*, 2230–2239. [[CrossRef](#)]
93. Szalontai, B.; Jakab, G. Differential expression of *PRLIPs*, a pathogenesis-related gene family encoding class 3 lipase-like proteins in Arabidopsis. *Acta Biol. Hung.* **2010**, *61* (Suppl. 1), 156–171. [[CrossRef](#)] [[PubMed](#)]
94. Nakano, R.T.; Piślewska-Bednarek, M.; Yamada, K.; Edger, P.P.; Miyahara, M.; Kondo, M.; Böttcher, C.; Mori, M.; Nishimura, M.; Schulze-Lefert, P.; et al. PYK10 myrosinase reveals a functional coordination between endoplasmic reticulum bodies and glucosinolates in *Arabidopsis thaliana*. *Plant J.* **2017**, *89*, 204–220. [[CrossRef](#)] [[PubMed](#)]
95. Chen, H.-Y.; Hsieh, E.-J.; Cheng, M.-C.; Chen, C.-Y.; Hwang, S.-Y.; Lin, T.-P. ORA47 (octadecanoid-responsive AP2/ERF-domain transcription factor 47) regulates jasmonic acid and abscisic acid biosynthesis and signaling through binding to a novel *cis*-element. *New Phytol.* **2016**, *211*, 599–613. [[CrossRef](#)]
96. Hickman, R.; Van Verk, M.C.; Van Dijken, A.J.H.; Pereira Mendes, M.; Vroegop-Vos, I.A.; Caarls, L.; Steenbergen, M.; Van der Nagel, I.; Wesselink, G.J.; Jironkin, A.; et al. Architecture and dynamics of the jasmonic acid gene regulatory network. *Plant Cell* **2017**, *29*, 2086–2105. [[CrossRef](#)]
97. Koo, A.J.K.; Howe, G.A. Role of peroxisomal β -oxidation in the production of plant signaling compounds. *Plant Signal. Behav.* **2007**, *2*, 20–22. [[CrossRef](#)]

98. Cheng, Z.; Sun, L.; Qi, T.; Zhang, B.; Peng, W.; Liu, Y.; Xie, D. The bHLH transcription factor MYC3 interacts with the jasmonate ZIM-domain proteins to mediate jasmonate response in *Arabidopsis*. *Mol. Plant* **2011**, *4*, 279–288. [[CrossRef](#)] [[PubMed](#)]
99. Niu, Y.; Figueroa, P.; Browse, J. Characterization of JAZ-interacting bHLH transcription factors that regulate jasmonate responses in *Arabidopsis*. *J. Exp. Bot.* **2011**, *62*, 2143–2154. [[CrossRef](#)]
100. Thireault, C.; Shyu, C.; Yoshida, Y.; St. Aubin, B.; Campos, M.L.; Howe, G.A. Repression of jasmonate signaling by a non-TIFY JAZ protein in *Arabidopsis*. *Plant J.* **2015**, *82*, 669–679. [[CrossRef](#)]
101. Fernández-Milmanda, G.L.; Crocco, C.D.; Reichelt, M.; Mazza, C.A.; Köllner, T.G.; Zhang, T.; Cargnel, M.D.; Lichy, M.Z.; Fiorucci, A.-S.; Fankhauser, C.; et al. A light-dependent molecular link between competition cues and defence responses in plants. *Nat. Plants* **2020**, *6*, 223–230. [[CrossRef](#)]
102. Koo, A.J.; Cooke, T.F.; Howe, G.A. Cytochrome P450 CYP94B3 mediates catabolism and inactivation of the plant hormone jasmonoyl-L-isoleucine. *Proc. Natl. Acad. Sci. USA* **2011**, *108*, 9298–9303. [[CrossRef](#)]
103. Bruckhoff, V.; Haroth, S.; Feussner, K.; König, S.; Brodhun, F.; Feussner, I. Functional characterization of CYP94-genes and identification of a novel jasmonate catabolite in flowers. *PLoS ONE* **2016**, *11*, e0159875. [[CrossRef](#)]
104. Poudel, A.N.; Holtsclaw, R.E.; Kimberlin, A.; Sen, S.; Zeng, S.; Joshi, T.; Lei, Z.; Sumner, L.W.; Singh, K.; Matsuura, H.; et al. 12-Hydroxy-jasmonoyl-L-isoleucine is an active jasmonate that signals through CORONATINE INSENSITIVE 1 and contributes to the wound response in *Arabidopsis*. *Plant Cell Physiol.* **2019**, *60*, 2152–2166. [[CrossRef](#)] [[PubMed](#)]
105. Zhu, Z.; Lee, B. Friends or foes: New insights in jasmonate and ethylene co-actions. *Plant Cell Physiol.* **2015**, *56*, 414–420. [[CrossRef](#)]
106. Caarls, L.; Pieterse, C.M.J.; Van Wees, S.C.M. How salicylic acid takes transcriptional control over jasmonic acid signaling. *Front. Plant Sci.* **2015**, *6*, 170. [[CrossRef](#)]
107. Torrens-Spence, M.P.; Bobokalonova, A.; Carballo, V.; Glinkerman, C.M.; Pluskal, T.; Shen, A.; Weng, J.-K. PBS3 and EPS1 complete salicylic acid biosynthesis from isochorismate in *Arabidopsis*. *Mol. Plant* **2019**, *12*, 1577–1586. [[CrossRef](#)]
108. Zwicker, S.; Mast, S.; Stos, V.; Pfitzner, A.J.P.; Pfitzner, U.M. Tobacco NIMIN2 proteins control PR gene induction through transient repression early in systemic acquired resistance. *Mol. Plant Pathol.* **2007**, *8*, 385–400. [[CrossRef](#)]
109. Kim, K.-C.; Lai, Z.; Fan, B.; Chen, Z. *Arabidopsis* WRKY38 and WRKY62 transcription factors interact with histone deacetylase 19 in basal defense. *Plant Cell* **2008**, *20*, 2357–2371. [[CrossRef](#)]
110. Hermann, M.; Maier, F.; Masroor, A.; Hirth, S.; Pfitzner, A.J.P.; Pfitzner, U.M. The *Arabidopsis* NIMIN proteins affect NPR1 differentially. *Front. Plant Sci.* **2013**, *4*, 88. [[CrossRef](#)] [[PubMed](#)]
111. Spoel, S.H.; van Ooijen, G. Circadian redox signaling in plant immunity and abiotic stress. *Antioxid. Redox Signal.* **2014**, *20*, 3024–3039. [[CrossRef](#)]
112. Hilker, M.; Fatouros, N.E. Plant responses to insect egg deposition. *Annu. Rev. Entomol.* **2015**, *60*, 493–515. [[CrossRef](#)]
113. Ojeda-Martinez, D.; Martinez, M.; Diaz, I.; Estrella Santamaria, M. Spider mite egg extract modifies *Arabidopsis* response to future infestations. *Sci. Rep.* **2021**, *11*, 17692. [[CrossRef](#)] [[PubMed](#)]
114. Danquah, A.; de Zelicourt, A.; Boudsocq, M.; Neubauer, J.; Frei dit Frey, N.; Leonhardt, N.; Pateyron, S.; Gwinner, F.; Tamby, J.P.; Ortiz-Masia, D.; et al. Identification and characterization of an ABA-activated MAP kinase cascade in *Arabidopsis thaliana*. *Plant J.* **2015**, *82*, 232–244. [[CrossRef](#)]
115. Sözen, C.; Schenk, S.T.; Boudsocq, M.; Chardin, C.; Almeida-Trapp, M.; Krapp, A.; Hirt, H.; Mithöfer, A.; Colcombet, J. Wounding and insect feeding trigger two independent MAPK pathways with distinct regulation and kinetics. *Plant Cell* **2020**, *32*, 1988–2003. [[CrossRef](#)]
116. Bar, M.; Shtein, I. Plant trichomes and the biomechanics of defense in various systems, with Solanaceae as a model. *Botany* **2019**, *97*, 651–660. [[CrossRef](#)]
117. Frerigmann, H.; Böttcher, C.; Baatout, D.; Gigolashvili, T. Glucosinolates are produced in trichomes of *Arabidopsis thaliana*. *Front. Plant Sci.* **2012**, *3*, 242. [[CrossRef](#)]
118. Zhou, L.H.; Liu, S.B.; Wang, P.F.; Lu, T.J.; Xu, F.; Genin, G.M.; Pickard, B.G. The *Arabidopsis* trichome is an active mechanosensory switch. *Plant Cell Environ.* **2017**, *40*, 611–621. [[CrossRef](#)] [[PubMed](#)]
119. Matsumura, M.; Nomoto, M.; Itaya, T.; Aratani, Y.; Iwamoto, M.; Matsuura, T.; Hayashi, Y.; Mori, T.; Skelly, M.J.; Yamamoto, Y.Y.; et al. Mechanosensory trichome cells evoke a mechanical stimuli-induced immune response in *Arabidopsis thaliana*. *Nat. Commun.* **2022**, *13*, 1216. [[CrossRef](#)]
120. Morohashi, K.; Grotewold, E. A systems approach reveals regulatory circuitry for *Arabidopsis* trichome initiation by the GL3 and GL1 selectors. *PLoS Genet.* **2009**, *5*, e1000396. [[CrossRef](#)]
121. Zhou, L.-L.; Shi, M.-Z.; Xie, D.-Y. Regulation of anthocyanin biosynthesis by nitrogen in TTG1-GL3/TT8-PAP1-programmed red cells of *Arabidopsis thaliana*. *Planta* **2012**, *236*, 825–837. [[CrossRef](#)]
122. Wen, J.; Li, Y.; Qi, T.; Gao, H.; Liu, B.; Zhang, M.; Huang, H.; Song, S. The C-terminal domains of *Arabidopsis* GL3/EGL3/TT8 interact with JAZ proteins and mediate dimeric interactions. *Plant Signal. Behav.* **2018**, *13*, 1795–1814. [[CrossRef](#)]
123. Yoshida, Y.; Sano, R.; Wada, T.; Takabayashi, J.; Okada, K. Jasmonic acid control of GLABRA3 links inducible defense and trichome patterning in *Arabidopsis*. *Development* **2009**, *136*, 1039–1048. [[CrossRef](#)] [[PubMed](#)]
124. Simmonds, M.S.J. Importance of flavonoids in insect-plant interactions: Feeding and oviposition. *Phytochemistry* **2001**, *56*, 245–252. [[CrossRef](#)] [[PubMed](#)]
125. Ramarosan, M.-L.; Koutouan, C.; Helesbeux, J.-J.; Le Clerc, V.; Hamama, L.; Geoffriau, E.; Briard, M. Role of phenylpropanoids and flavonoids in plant resistance to pests and diseases. *Molecules* **2022**, *27*, 8371. [[CrossRef](#)] [[PubMed](#)]

126. Bariola, P.A.; MacIntosh, G.C.; Green, P.J. Regulation of S-like ribonuclease levels in *Arabidopsis*. Antisense inhibition of *RNS1* or *RNS2* elevates anthocyanin accumulation. *Plant Physiol.* **1999**, *119*, 331–342. [[CrossRef](#)] [[PubMed](#)]
127. Agati, G.; Brunetti, C.; Fini, A.; Gori, A.; Guidi, L.; Landi, M.; Sebastiani, F.; Tattini, M. Are flavonoids effective antioxidants in plants? Twenty years of our investigation. *Antioxidants* **2020**, *9*, 1098. [[CrossRef](#)] [[PubMed](#)]
128. Xiao, Y.; Wang, Q.; Erb, M.; Turlings, T.C.J.; Ge, L.; Hu, L.; Li, J.; Han, X.; Zhang, T.; Lu, J.; et al. Specific herbivore-induced volatiles defend plants and determine insect community composition in the field. *Ecol. Lett.* **2012**, *15*, 1130–1139. [[CrossRef](#)] [[PubMed](#)]
129. Turlings, T.C.J.; Erb, M. Tritrophic interactions mediated by herbivore-induced plant volatiles: Mechanisms, ecological relevance, and application potential. *Annu. Rev. Entomol.* **2018**, *63*, 433–452. [[CrossRef](#)] [[PubMed](#)]
130. Gurr, G.M.; Liu, J.; Pickett, J.A.; Stevenson, P.C. Review of the chemical ecology of homoterpenes in arthropod-plant interactions. *Austral Entomol.* **2023**, *62*, 2–14. [[CrossRef](#)]
131. Ehrling, J.; Chowrira, S.G.; Mattheus, N.; Aeschliman, D.S.; Arimura, G.I.; Bohlmann, J. Comparative transcriptome analysis of *Arabidopsis thaliana* infested by diamond back moth (*Plutella xylostella*) larvae reveals signatures of stress response, secondary metabolism, and signalling. *BMC Genom.* **2008**, *9*, 154. [[CrossRef](#)]
132. Herde, M.; Gartner, K.; Kollner, T.G.; Fode, B.; Boland, W.; Gershenzon, J.; Gatz, C.; Tholl, D. Identification and regulation of TPS04/GES, an *Arabidopsis* geranylinalool synthase catalyzing the first step in the formation of the insect-induced volatile C₁₆-homoterpene TMTT. *Plant Cell* **2008**, *20*, 1152–1168. [[CrossRef](#)]
133. Schweizer, F.; Bodenhausen, N.; Lassueur, S.; Masclaux, F.G.; Reymond, P. Differential contribution of transcription factors to *Arabidopsis thaliana* defense against *Spodoptera littoralis*. *Front. Plant Sci.* **2013**, *4*, 13. [[CrossRef](#)] [[PubMed](#)]
134. Kroes, A.; Broekgaarden, C.; Castellanos Uribe, M.; May, S.; van Loon, J.J.; Dicke, M. *Brevicoryne brassicae* aphids interfere with transcriptome responses of *Arabidopsis thaliana* to feeding by *Plutella xylostella* caterpillars in a density-dependent manner. *Oecologia* **2017**, *183*, 107–120. [[CrossRef](#)] [[PubMed](#)]
135. Williams III, L.; Rodriguez-Saona, C.; Castle, S.C.; Zhu, S. EAG-active herbivore-induced plant volatiles modify behavioral responses and host attack by an egg parasitoid. *J. Chem. Ecol.* **2008**, *34*, 1190–1201. [[CrossRef](#)] [[PubMed](#)]
136. Krugner, R.; Wallis, C.M.; Walse, S.S. Attraction of the egg parasitoid, *Gonatocerus ashmeidi* Giralt (Hymenoptera: Mymaridae) to synthetic formulation of a (*E*)- β -ocimene and (*E,E*)- α -farnesene mixture. *Biol. Control* **2014**, *77*, 23–28. [[CrossRef](#)]
137. Morawo, T.; Fadamiro, H. Identification of key plant-associated volatiles emitted by *Heliothis virescens* larvae that attract the parasitoid *Microplitis croceipes*: Implications for parasitoid perception of odor blends. *J. Chem. Ecol.* **2016**, *42*, 1112–1121. [[CrossRef](#)] [[PubMed](#)]
138. Lin, J.; Wang, D.; Chen, X.; Köllner, T.G.; Mazareim, M.; Guo, H.; Pantalone, V.R.; Arelli, P.; Stewart, C.N., Jr.; Wang, N.; et al. An (*E,E*)- α -farnesene synthase genes of soybean has a role in defence against nematodes and is involved in synthesizing insect-induced volatiles. *Plant Biotechnol. J.* **2017**, *15*, 510–519. [[CrossRef](#)] [[PubMed](#)]
139. Nurkomar, I.; Pudjianto; Manuwoto, S.; Buchori, D.; Matsuyama, S.; Taylor, D.; Kainoh, Y. (*E,E*)- α -farnesene as a host-induced plant volatile that attracts *Apanteles taragamae* (Hymenoptera: Braconidae) to host-infested cucumber plants. *Biocontrol Sci. Technol.* **2018**, *28*, 34–48. [[CrossRef](#)]
140. Matthes, M.C.; Bruce, T.J.A.; Ton, J.; Verrier, P.J.; Pickett, J.A.; Napier, J.A. The transcriptome of *cis*-jasmonate-induced resistance in *Arabidopsis thaliana* and its role in indirect defence. *Planta* **2010**, *232*, 1163–1180. [[CrossRef](#)]
141. Bodenhausen, N.; Reymond, P. Signaling pathways controlling induced resistance to insect herbivores in *Arabidopsis*. *Mol. Plant-Microbe Interact.* **2007**, *20*, 1406–1420. [[CrossRef](#)]
142. Duan, H.; Huang, M.Y.; Palacio, K.; Schuler, M.A. Variations in *CYP74B2* (Hydroperoxide lyase) gene expression differentially affect hexenal signaling in the Columbia and Landsberg *erecta* ecotypes of *Arabidopsis*. *Plant Physiol.* **2005**, *139*, 1529–1544. [[CrossRef](#)]
143. Snoeren, T.A.L.; Mumm, R.; Poelman, E.H.; Yang, Y.; Pichersky, E.; Dicke, M. The herbivore-induced plant volatiles methyl salicylate negatively affects attraction of the parasitoid *Diadegma semiclausum*. *J. Chem. Ecol.* **2010**, *36*, 479–489. [[CrossRef](#)] [[PubMed](#)]
144. Groux, R.; Hilfiker, O.; Gouhier-Darimont, C.; Gomes Villalba Penafior, M.F.; Erb, M.; Reymond, P. Role of methyl salicylate on oviposition deterrence in *Arabidopsis thaliana*. *J. Chem. Ecol.* **2014**, *40*, 754–759. [[CrossRef](#)] [[PubMed](#)]
145. Kroes, A.; Weldegergis, B.T.; Cappai, F.; Dicke, M.; van Loon, J.J.A. Terpenoid biosynthesis in *Arabidopsis* attacked by caterpillars and aphids: Effects of aphid density on the attraction of a caterpillar parasitoid. *Oecologia* **2017**, *185*, 699–712. [[CrossRef](#)] [[PubMed](#)]
146. Wei, J.; Kang, L. Roles of (*Z*)-3-hexenol in plant-insect interactions. *Plant Signal. Behav.* **2011**, *6*, 369–371. [[CrossRef](#)] [[PubMed](#)]
147. Kishimoto, K.; Matsui, K.; Ozawa, R.; Takabayashi, J. Volatile C₆-aldehydes and allo-ocimene activate defense genes and induce resistance against *Botrytis cinerea* in *Arabidopsis thaliana*. *Plant Cell Physiol.* **2005**, *46*, 1093–1102. [[CrossRef](#)] [[PubMed](#)]
148. Hirao, T.; Okazawa, A.; Harada, K.; Kobayashi, A.; Muranaka, T.; Hirata, K. Green leaf volatiles enhance methyl jasmonate response in *Arabidopsis*. *J. Biosci. Bioeng.* **2012**, *114*, 540–545. [[CrossRef](#)] [[PubMed](#)]
149. Rosenkranz, M.; Chen, Y.; Zhu, P.; Vlot, A.C. Volatile terpenes—Mediators of plant-to-plant communication. *Plant J.* **2021**, *108*, 617–631. [[CrossRef](#)] [[PubMed](#)]
150. Fagan, W.F.; Siemann, E.; Mitter, C.; Denno, R.F.; Huberty, A.F.; Woods, H.A.; Elser, J.J. Nitrogen in insects: Implications for trophic complexity and species diversification. *Am. Nat.* **2002**, *160*, 784–802. [[CrossRef](#)] [[PubMed](#)]

151. Holtorf, M.; Lenaerts, C.; Cullen, D.; Vanden Broeck, J. Extracellular nutrient digestion and absorption in the insect gut. *Cell Tissue Res.* **2019**, *377*, 397–414. [[CrossRef](#)] [[PubMed](#)]
152. Jongasma, M.A.; Beekwilder, J. Co-evolution of insect proteases and plant protease inhibitors. *Curr. Protein Pept. Sci.* **2011**, *12*, 437–447. [[CrossRef](#)]
153. Sultana, M.S.; Mazarei, M.; Jurat-Fuentes, J.L.; Hewezi, T.; Millwood, R.J.; Stewart, C.N. Overexpression of soybean trypsin inhibitor genes decreases defoliation by corn earworm (*Helicoverpa zea*) in soybean (*Glycine max*) and *Arabidopsis thaliana*. *Front. Plant Sci.* **2023**, *14*, 370. [[CrossRef](#)]
154. Kuśnierczyk, A.; Winge, P.; Midelfart, H.; Armbruster, W.S.; Rossiter, J.T.; Bones, A.M. Transcriptional responses of *Arabidopsis thaliana* ecotypes with different glucosinolate profiles after attack by polyphagous *Myzus persicae* and oligophagous *Brevicoryne brassicae*. *J. Exp. Bot.* **2007**, *58*, 2537–2552. [[CrossRef](#)]
155. Adio, A.M.; Casteel, C.L.; De Vos, M.; Kim, J.H.; Joshi, V.; Li, B.; Juery, C.; Daron, J.; Kliebenstein, D.J.; Jander, G. Biosynthesis and defensive function of N δ -acetylornithine, a jasmonate-induced *Arabidopsis* metabolite. *Plant Cell* **2011**, *23*, 3303–3318. [[CrossRef](#)]
156. Taylor, N.L.; Howell, K.A.; Heazlewood, J.L.; Tan, T.Y.W.; Narsai, R.; Huang, S.; Whelan, J.; Millar, A.H. Analysis of the rice mitochondrial carrier family reveals anaerobic accumulation of a basic amino acid carrier involved in arginine metabolism during seed germination. *Plant Physiol.* **2010**, *154*, 691–704. [[CrossRef](#)]
157. Dow, J.A. pH gradients in lepidopteran midgut. *J. Exp. Biol.* **1992**, *172*, 355–375. [[CrossRef](#)]
158. Flores, T.; Todd, C.D.; Tovar-Mendez, A.; Dhanoa, P.K.; Correa-Aragunde, N.; Hoyos, M.E.; Brownfield, D.M.; Mullen, R.T.; Lamattina, L.; Polacco, J.C. Arginase-negative mutants of *Arabidopsis* exhibit increased nitric oxide signaling in root development. *Plant Physiol.* **2008**, *147*, 1936–1946. [[CrossRef](#)] [[PubMed](#)]
159. Foresci, N.; Correa-Aragunde, N.; Parisi, G.; Caló, G.; Salerno, G.; Lamattina, L. Characterization of a nitric oxide synthase from the plant kingdom: NO generation from the green alga *Ostreococcus tauri* is light irradiance and growth phase dependent. *Plant Cell* **2010**, *22*, 381603830. [[CrossRef](#)] [[PubMed](#)]
160. Winter, G.; Todd, C.D.; Trovato, M.; Forlani, G.; Funck, D. Physiological implications of arginine metabolism in plants. *Front. Plant Sci.* **2015**, *6*, 534. [[CrossRef](#)] [[PubMed](#)]
161. Kolbert, Z.; Barroso, J.B.; Brouquisse, R.; Corpas, F.J.; Gupta, K.J.; Lindermayr, C.; Loake, G.J.; Palma, J.M.; Petřivalský, M.; Wendehennem, D.; et al. A forty year journey: The generation and roles of NO in plants. *Nitric Oxide* **2019**, *93*, 53–70. [[CrossRef](#)]
162. Wünsche, H.; Baldwin, I.T.; Wu, J. S-Nitrosoglutathione reductase (GSNOR) mediates the biosynthesis of jasmonic acid and ethylene induced by feeding of the insect herbivore *Manduca sexta* and is important for jasmonate-elicited responses in *Nicotiana attenuata*. *J. Exp. Bot.* **2011**, *62*, 4605–4616. [[CrossRef](#)]
163. Espunya, M.C.; De Michele, R.; Gomez-Cadenas, A.; Martínez, M.C. S-Nitrosoglutathione is a component of wound- and salicylic acid-induced systemic responses in *Arabidopsis thaliana*. *J. Exp. Bot.* **2012**, *63*, 3219–3227. [[CrossRef](#)]
164. Hu, J.; Huang, X.; Chen, L.; Sun, X.; Lu, C.; Zhang, L.; Wang, Y.; Zuo, J. Site-specific nitrosoproteomic identification of endogenously S-nitrosylated proteins in *Arabidopsis*. *Plant Physiol.* **2015**, *167*, 1731–1746. [[CrossRef](#)]
165. Feng, J.; Chen, L.; Zuo, J. Protein S-nitrosylation in plants: Current progresses and challenges. *J. Integr. Plant Biol.* **2019**, *61*, 1206–1223. [[CrossRef](#)] [[PubMed](#)]
166. Santamaria, M.E.; Martínez, M.; Arnaiz, A.; Rioja, C.; Burow, M.; Grbic, V.; Díaz, I. An *Arabidopsis* TIR-lectin two-domain protein confers defense properties against *Tetranychus urticae*. *Plant Physiol.* **2019**, *179*, 1298–1314. [[CrossRef](#)]
167. Michiels, K.; Van Damme, E.J.; Smagghe, G. Plant-insect interactions: What can we learn from plant lectins? *Arch. Insect Biochem. Physiol.* **2010**, *73*, 193–212. [[CrossRef](#)] [[PubMed](#)]
168. Beneteau, J.; Renard, D.; Marché, L.; Douville, E.; Lavenant, L.; Rahbé, Y.; Dupont, D.; Vilaine, F.; Dinant, S. Binding properties of the N-acetylglucosamine and high-mannose N-glycan PP2-A1 phloem lectin in *Arabidopsis*. *Plant Physiol.* **2010**, *153*, 1345–1361. [[CrossRef](#)]
169. Zhang, C.; Shi, H.; Chen, L.; Wang, X.; Lü, B.; Zhang, S.; Liang, Y.; Liu, R.; Qian, J.; Sun, W.; et al. Harpin-induced expression and transgenic overexpression of the phloem protein gene *AtPP2-A1* in *Arabidopsis* repress phloem feeding of the green peach aphid *Myzus persicae*. *BMC Plant Biol.* **2011**, *11*, 11. [[CrossRef](#)] [[PubMed](#)]
170. Kariola, T.; Brader, G.; Li, J.; Palva, E.T. Chlorophyllase 1, a damage control enzyme, affects the balance between defense pathways in plants. *Plant Cell* **2005**, *17*, 282–294. [[CrossRef](#)]
171. Pospíšil, P. Molecular mechanisms of production and scavenging of reactive oxygen species by photosystem II. *Biochim. Biophys. Acta* **2012**, *1817*, 218–231. [[CrossRef](#)]
172. Hu, X.; Makita, S.; Schelbert, S.; Sano, S.; Ochiai, M.; Tsuchiya, T.; Hasegawa, S.F.; Hörtensteiner, S.; Tanaka, A.; Tanaka, R. Reexamination of chlorophyllase function implies its involvement in defense against chewing herbivores. *Plant Physiol.* **2015**, *167*, 660–670. [[CrossRef](#)]
173. Pandian, G.N.; Ishikawa, T.; Togashi, M.; Shitomi, Y.; Haginoya, K.; Yamamoto, S.; Nishiumi, T.; Hori, H. *Bombyx mori* midgut membrane protein P252, which binds to *Bacillus thuringiensis* Cry1A, is a chlorophyllide-binding protein, and the resulting complex has antimicrobial activity. *Appl. Environ. Microbiol.* **2008**, *74*, 1324–1331. [[CrossRef](#)] [[PubMed](#)]
174. Boyes, D.C.; Zayed, A.M.; Ascenzi, R.; McCaskill, A.J.; Hoffman, N.E.; Davis, K.R.; Gorch, J. Growth stage-based phenotypic analysis of *Arabidopsis*: A model for high throughput functional genomics in plants. *Plant Cell* **2001**, *13*, 1499–1510. [[CrossRef](#)] [[PubMed](#)]

175. Martinez Henao, J.; Demers, L.E.; Grosser, K.; Schedl, A.; Van Dam, N.M.; Bede, J.C. Fertilizer rate-associated increase in foliar jasmonate burst observed in wounded *Arabidopsis thaliana* leaves is attenuated at eCO₂. *Front. Plant Sci.* **2020**, *10*, 1636. [[CrossRef](#)] [[PubMed](#)]
176. Grosser, K.; van Dam, N.M. A straightforward method for glucosinolate extraction and analysis with high-pressure liquid chromatography (HPLC). *J. Vis. Exp.* **2017**, *121*, e55425. [[CrossRef](#)]
177. Andrews, S.; Krueger, F.; Segonds-Pichon, A.; Biggins, L.; Krueger, C.; Wingett, S. FastQC: A Quality Control Tool for High Throughput Sequence Data. 2010. Available online: <http://www.bioinformatics.babraham.ac.uk/projects/fastqc/> (accessed on 1 August 2022).
178. Chen, S.; Zhou, Y.; Chen, Y.; Gu, J. Fastp: An ultra-fast all-in-one FASTQ preprocessor. *Bioinformatics* **2018**, *34*, i884–i890. [[CrossRef](#)] [[PubMed](#)]
179. Dobin, A.; Davis, C.A.; Schlesinger, F.; Drenkow, J.; Zaleski, C.; Jha, S.; Batut, P.; Chaisson, M.; Gingeras, T.R. STAR: Ultrafast universal RNA-seq aligner. *Bioinformatics* **2013**, *29*, 15–21. [[CrossRef](#)] [[PubMed](#)]
180. Zhou, G.; Soufan, O.; Ewald, J.; Hancock, R.E.W.; Basu, N.; Xia, J. NetworkAnalyst 3.0: A visual analytics platform for comprehensive gene expression profiling and meta-analysis. *Nucleic Acids Res.* **2019**, *47*, W234–W241. [[CrossRef](#)]
181. Love, M.I.; Huber, W.; Anders, S. Moderated estimation of fold change and dispersion for RNA-Seq data with DESeq2. *Genome Biol.* **2014**, *15*, 550. [[CrossRef](#)] [[PubMed](#)]
182. Zhu, A.; Ibrahim, J.G.; Love, M.I. Heavy-tailed prior distributions for sequence count data: Removing the noise and preserving large differences. *Bioinformatics* **2019**, *35*, 2084–2092. [[CrossRef](#)]
183. Pang, Z.; Chong, J.; Zhou, G.; de Lima Morais, D.A.; Chang, L.; Barrette, M.; Gauthier, C.; Jacques, P.-É.; Li, S.; Xia, J. MetaboAnalyst 5.0: Narrowing the gap between raw spectra and functional insights. *Nucleic Acids Res.* **2021**, *49*, W389. [[CrossRef](#)]
184. Ewald, J.; Zhou, G.; Lu, Y.; Xia, J. Using ExpressAnalyst for comprehensive gene expression analysis in model and non-model organisms. *Curr. Protoc.* **2023**, *3*, e922. [[CrossRef](#)] [[PubMed](#)]

Disclaimer/Publisher’s Note: The statements, opinions and data contained in all publications are solely those of the individual author(s) and contributor(s) and not of MDPI and/or the editor(s). MDPI and/or the editor(s) disclaim responsibility for any injury to people or property resulting from any ideas, methods, instructions or products referred to in the content.